

**EFFECT OF MICRON AND NANO  $\text{MgAl}_2\text{O}_4$  SPINEL  
ADDITION ON THE PROPERTIES OF MAGNESIA-CARBON  
REFRACTORIES**

A THESIS SUBMITTED IN PARTIAL FULFILLMENT OF THE  
REQUIREMENTS FOR THE DEGREE OF

**Master of Technology (Research)**  
**in**  
**Ceramic Engineering**

By  
**RASHMI REKHA DAS**



**Department of Ceramic Engineering**  
**National Institute of Technology**  
**Rourkela**

October 2010

**EFFECT OF MICRON AND NANO  $\text{MgAl}_2\text{O}_4$  SPINEL  
ADDITION ON THE PROPERTIES OF MAGNESIA-CARBON  
REFRACTORIES**

A THESIS SUBMITTED IN PARTIAL FULFILLMENT OF THE  
REQUIREMENTS FOR THE DEGREE OF

**Master of Technology (Research)**  
**in**  
**Ceramic Engineering**

By  
**RASHMI REKHA DAS**

Under the Guidance of  
**Dr. Bibhuti Bhusan Nayak**  
**and**  
**Dr. Sukumar Adak**



**Department of Ceramic Engineering**  
**National Institute of Technology**  
**Rourkela**

October 2010



**National Institute of Technology**  
**Rourkela**

**CERTIFICATE**

This is to certify that the thesis entitled, "Effect of micron and nano  $\text{MgAl}_2\text{O}_4$  spinel addition on the properties of magnesia-carbon refractories" submitted by Mrs. Rashmi Rekha Das in partial fulfillments of the requirements for the award of Master of Technology (Research) Degree in Ceramic Engineering at National Institute of Technology, Rourkela is an authentic work carried out by her under our supervision and guidance.

To the best of our knowledge, the matter embodied in the thesis has not been submitted to any other University / Institute for the award of any Degree or Diploma.

Dr. Sukumar Adak  
Vice President (Technology)  
Tata Refractories Limited  
Belpahar  
Orissa-768 218

Dr. Bibhuti Bhusan Nayak  
Associate Professor  
Dept. of Ceramic Engineering  
National Institute of Technology, Rourkela  
Orissa – 769 008

Date: 25/10/2010

# CONTENTS

	Page No
<i>Abstract</i>	<i>i</i>
<i>Acknowledgements</i>	<i>ii</i>
<i>List of Figures</i>	<i>iii</i>
<i>List of Tables</i>	<i>iv</i>
<b>Chapter 1            GENERAL INTRODUCTION</b>	<b>1-8</b>
1.1 Introduction	2
1.2 MgO-C refractory and its application in ladle	3
1.3 Role of spinel in MgO-C refractory	5
1.4 Role of ceramic nanoparticles in refractory industry	6
1.5 Organization of the thesis	8
<b>Chapter 2            LITERATURE REVIEW</b>	<b>9-22</b>
2.1 Technological evolution of MgO-C refractories	10
2.2 Selection of raw materials	11
2.3 Role of micron-sized, stoichiometric and in-situ spinel in MgO-C brick	15
2.4 Mechanisms of corrosion in MgO-C bricks	17
2.5 Effect of nanoparticles on the properties of MgO-C refractories	19
2.6 Synthesis of MgAl <sub>2</sub> O <sub>4</sub> spinel using different chemical routes	20
2.7 Summary of literature	21
2.8 Objectives of the present studies	22
<b>Chapter 3            EXPERIMENTAL WORK</b>	<b>23-32</b>
3.1 Raw materials and fabrication of micron and nano spinel added MgO-C brick	24
3.2 Synthesis of MgAl <sub>2</sub> O <sub>4</sub> spinel nanopowders	27
3.3 General Characterization	28
3.3.1 AP, BD and CCS	28
3.3.2 HMOR	28
3.3.3 MOE	29
3.3.4 TSI	29
3.3.5 Oxidation resistance	29
3.3.6 Rotary slag corrosion test for micron sized spinel added MgO-C bricks	30
3.3.7 Static crucible slag corrosion test for nano sized spinel added MgO-C bricks	31
3.3.8 Pore size distribution	31
3.3.9 Thermal	31
3.3.10 Surface area	31
3.3.11 Phase analysis	32
3.3.12 Microstructure	32

<b>Chapter 4</b>	<b>RESULTS AND DISCUSSION</b>	33-54
<b>4.1</b>	<b>Physical and chemical properties of micron-sized <math>\text{MgAl}_2\text{O}_4</math> spinel added MgO-C bricks</b>	34
4.1.1	AP, BD and CCS (before and after coking)	34
4.1.2	HMOR and TSI	35
4.1.3	Oxidation resistance	37
4.1.4.	Rotary slag corrosion	38
4.1.5	Corrosion	39
4.1.6	Pore size distribution	40
4.1.7	Microstructure	41
4.1.8	Summary	44
<b>4.2</b>	<b>Characterization of <math>\text{MgAl}_2\text{O}_4</math> spinel nanopowders synthesized by citrate-nitrate method</b>	45
4.2.1.	Thermal analysis	45
4.2.2.	Structure and microstructure	46
4.2.3	Surface area	47
4.2.4	Summary	47
<b>4.3</b>	<b>Physical and chemical properties of without, standardized and nano-sized <math>\text{MgAl}_2\text{O}_4</math> spinel added MgO-C refractory</b>	48
4.3.1	AP, BD and CCS (before and after coking)	48
4.3.2	HMOR and TSI	49
4.3.3	Oxidation resistance	50
4.3.4.	Static crucible slag corrosion	50
4.3.5	Corrosion	51
4.3.6	Pore size distribution	53
4.3.7	Microstructure	53
4.3.8	Summary	54
<b>Chapter 5</b>	<b>CONCLUSIONS</b>	55-57
	SCOPE FOR FUTURE WORK	57
	References	58-69
	Curriculum Vitae	

## ABSTRACT

Magnesia- carbon (MgO-C) refractory bricks have been used in the slag line of ladles due to its superior slag penetration resistance and excellent thermal shock resistance at high temperatures. However, the life of this bricks has become limited on prolonged use due to its poor oxidation resistance as well as low strength at high temperatures. Thus, the physical and chemical properties of MgO-C refractories could be improved by the addition of suitable additives in micron or nano range. Magnesium aluminate ( $\text{MgAl}_2\text{O}_4$ ) spinel has been recognized as one of the most effective refractory material due to its excellent wear and slag resistance. The particle size distribution of  $\text{MgAl}_2\text{O}_4$  spinel is also important factor that influence both the physical and chemical properties of refractories. Hence, the present work deals with the improvement of the physical and chemical properties of MgO-C refractories with the addition of  $\text{MgAl}_2\text{O}_4$  spinel in micron and nano range.

In this work, a set of experiments was carried out in order to standardize the type and amount of preformed spinel addition in MgO-C refractory system. Here, micron-sized  $\text{MgAl}_2\text{O}_4$  spinel in three different commercially available grades such as near stoichiometric (AR-78), alumina rich (AR-90) and magnesia rich (MR-66) have been used during fabrication of MgO-C bricks. Micron-sized spinel added MgO-C bricks with sixteen compositions have been fabricated using different raw materials such as fused magnesia (FM97LC), flake graphite, resin, pitch and Al-metal powder. The micron spinel content was varied from 0 to 25 wt % with the incremental addition of 5 wt % in MgO-C bricks. It was observed that 10% AR-78 spinel added MgO-C bricks exhibits better corrosion and oxidation resistance as compared to that of AR-90 or MR-66 spinel added MgO-C bricks. HMOR and TSI were higher for AR-78 (10 wt %) spinel added MgO-C bricks. From the microstructure, it was observed that the dissolution of MgO grains into slag was less and carbon retention was more for AR-78 spinel added bricks as compared to without spinel added bricks. The standardized type and amount of spinel (10 wt % AR-78) was then taken in order to compare and carry out the second set of experiments. In this experiment, the effect of without, standardized micron-sized (10 wt % AR78) and nano-sized  $\text{MgAl}_2\text{O}_4$  spinel added MgO-C bricks properties are correlated.

Nano-sized  $\text{MgAl}_2\text{O}_4$  spinel has been prepared using citrate-nitrate method and calcined at 800 °C to get a cubic phase. These calcined spinel powders have been added with different weight percentage such as 0.1, 0.5, 1 and 1.5 in MgO-C bricks.

The average pore diameter of nano spinel added brick was lower as compared to AR-78 spinel added MgO-C bricks. Nano spinel addition restricts the dissolution of MgO grains and retains the carbon in the matrix. It was observed that with addition of 0.5 to 1 wt % nano  $\text{MgAl}_2\text{O}_4$  spinel gives better HMOR and TSI as well as oxidation and slag corrosion resistance as compared to 10 wt % AR-78 spinel added MgO-C brick.

Hence, the above results of the micron and nano  $\text{MgAl}_2\text{O}_4$  spinel added MgO-C bricks clearly show the potential application in the slag lines of ladle furnace.

---

**Keywords:** MgO-C refractories;  $\text{MgAl}_2\text{O}_4$ ; Nanopowders; Slag corrosion resistance; Oxidation resistance; Spinel.

## **ACKNOWLEDGEMENTS**

It is a pleasure to thank many people who made this thesis possible.

I have been indebted in the preparation of this thesis to my supervisors, Dr. Bibhuti Bhusan Nayak and Dr. Sukumar Adak, whose patience, kindness and academic experience has been a great value to me.

I would also like to take this opportunity to express my sincere thanks to faculty and staff members of Department of Ceramic Engineering, N.I.T., Rourkela, and my colleagues at Tata Refractories Limited, Belpahar.

Above all, I would like to thank my husband, Dr.M. Sathiyakumar who stood beside me for his encouragement throughout this entire journey, without whom I would have struggled to find the inspiration and motivation needed to complete this dissertation. Also I would like to express my heartfelt affection to my daughter S.R. Simran Saloni for giving me happiness and joy throughout this journey.

I wish to thank my parents, Mrs. Basanti Lata Das and Mr. Shyam Sundar Das, who have raised me, supported me, taught me, and loved me. To them I dedicate this thesis.

Finally, I would like to thank the Management of Tata Refractories Limited (TRL) for giving me an opportunity to pursue this study by sponsoring and providing me with all necessary help and support.

Date: 25/10/10

*Rashmi Rekha Das*  
(Rashmi Rekha Das)

## List of Figures

	Page No
Fig.1.1: Schematic view and various parts of steel ladle	04
Fig. 2.1: Different phenomena of corrosion in refractories	17
Fig. 2.2: Different penetration conditions of slag in refractory	18
Fig. 3.1: Schematic flow diagram for the preparation of $\text{MgAl}_2\text{O}_4$ spinel nanopowder	27
Fig.3.2: Rotary furnace for conducting slag corrosion test for micron-sized spinel added MgO-C bricks	30
Fig. 4.1: HMOR and TSI as a function of different types and amounts of micron-spinel added MgO-C bricks	37
Fig. 4.2: Black surface remaining in % after oxidation resistance test for different bricks	38
Fig. 4.3: Surface pattern of different spinel type MgO-C bricks after slag corrosion test	39
Fig. 4.4: Corrosion (mm) as a function of different spinel added MgO-C refractories	39
Fig. 4.5: Optical micrographs of (a) normal and (b) large crystal of 97 % fused MgO	41
Fig. 4.6: Optical micrographs of MgO-C bricks without spinel addition after slag corrosion test which indicate (a) Crack formation and (b) disintegration of MgO grains	42
Fig.4.7: Optical micrograph shows graphite intact for AR-78 spinel added MgO-C bricks after slag corrosion test	43
Fig. 4.8: Optical micrographs of MgO-C bricks (a) without spinel and (b) with AR-78 spinel after slag corrosion test	44
Fig. 4.9: DSC-TG curve of the gel	45
Fig.4.10: XRD patterns of as-prepared spinel nanopowders calcined at different temperatures	46
Fig.4.11: SEM micrograph of $\text{MgAl}_2\text{O}_4$ nanopowder	47
Fig. 4.12: HMOR and TSI as a function of spinel added MgO-C refractory	49
Fig. 4.13: Black surface remaining in % as a function of spinel addition in MgO-C refractory	50
Fig. 4.14: Surface pattern of different spinel type MgO-C samples after slag corrosion test	51
Fig. 4.15: Corrosion (mm) as a function of spinel added MgO-C refractories	52
Fig. 4.16: Optical micrographs of (a) 0.5 % and (b) 1 % nano spinel added MgO-C refractories after slag corrosion test	54



<b>List of Tables</b>	<b>Page No</b>
Table 1.1: Different working lining designs in steel ladles in India	04
Table 2.1: Technological evolution of MgO-C refractory	10
Table. 2.2: Chemical and physical properties of magnesia aggregate	12
Table 2.3: Characteristics of flake graphite used for carbon containing refractories	12
Table 2.4: Various routes for preparation of nano $\text{MgAl}_2\text{O}_4$ spinel	21
Table 3.1: Physical and chemical analysis of flake graphite	24
Table 3.2: Physical and chemical analysis of liquid resin and pitch powder	24
Table 3.3: Chemical composition in percentage of fused magnesia and spinel	25
Table 3.4: Batch composition of micron-sized spinel added MgO-C bricks	25
Table 3.5: Batch composition of nano spinel added MgO-C refractory	26
Table 3.6: Mixing sequence of MgO-C bricks	26
Table 3.7: Chemical composition (%) and basicity of the steel making ladle slag	30
Table 4.1: AP (before and after coking) of MgO-C refractories with addition of micron-sized spinel	34
Table 4.2: BD (before and after coking) of MgO-C refractories with addition of micron-sized spinel	34
Table 4.3: CCS (before and after coking) of MgO-C refractories with addition of micron-sized spinel	34
Table 4.4: Distribution of pores in MgO-C bricks after slag corrosion	40
Table 4.5: AP, BD and CCS of nano-sized $\text{MgAl}_2\text{O}_4$ spinel added MgO-C refractories, correlated with ZS and AR-78 added MgO-C refractories	48
Table 4.6: Distribution of pores in spinel added MgO-C refractories after slag corrosion	53

# **Chapter 1**

## *GENERAL INTRODUCTION*

## 1.1 Introduction

Refractories play an important role in metallurgical, glassmaking and ceramic industries, where they are formed into a variety of shapes to line the interiors of furnaces or kilns or other devices for processing the materials at high temperatures [1-2]. Many of the scientific and technological inventions and developments would not have been possible without refractory materials. Dreaming about producing one kilogram of any metal without the use of refractory is almost quite impossible. The ASTM C71 defines the refractories as "nonmetallic materials having those chemical and physical properties that make them applicable for structures or as components of systems that are exposed to environments above 1000 °F (538 °C)" [3].

The type of refractories to be used is often dictated by the conditions prevailing in the application area. Generally, refractories are classified into two different groups [4]: (a) based on raw materials, the refractories are subdivided into three categories such as acidic (zircon, fireclay and silica), basic (dolomite, magnesite, magnesia-carbon, chrome-magnesite and magnesite-chrome) and neutral (alumina, chromite, silicon carbide, carbon and mullite) and (b) based on manufacturing process, the refractories are subdivided into two categories such as shaped refractories (available in the form of different brick shapes, and includes the oxide and non-oxide systems) and unshaped refractories (which includes mortars, castables and monolithic).

In tune with the changing trends in steelmaking, especially in ladle metallurgy, the high performing shaped refractories are on an increasing demand in recent years. The higher campaign lives and the variability of newer steel making operations are decided by the availability and performance of such shaped refractories with superior high temperature mechanical strength, erosion and corrosion resistance [5]. Initially, the ladles were used only to transport the steel from steel making unit to casting bay, but now-a-days the refining process is also carried out in the same. Thus, steel producers throughout the world have been putting on a continuous effort to improve the ladle life in order to increase the performance of ladles as well as reduce the specific consumption of refractories so as to have a strong grip over cost and quality of steel and also to increase the ladle availability with lesser number of ladles relining per day [6]. Due to the above

reasons, there had been a great technological evolution in ladle lining concept such as: zonal lining concept, which deals with both selection of refractory quality and refractory lining thickness [7-10]. In today's scenario, it is quite impossible to imagine a steel teeming ladle without magnesia-carbon (MgO-C) refractory bricks. MgO-C bricks have dominated the slag line of ladles for at least a decade as they possess superior slag penetration resistance and excellent thermal shock resistance at elevated temperature because of the non-wetting property of carbon (graphite) with slag, high thermal conductivity, low thermal expansion and high toughness [11, 12]. However, the life of these refractories has become somewhat limited on prolonged use and increasing severity of operating condition due to its poor oxidation resistance as well as low strength at high temperatures [13]. The lining of ladle depends to a greater extent on the wear rate of MgO-C refractory arising from slag penetration and structural spalling. Increased steel production has led both refractory manufacturers and users to resume interest on further improvement of thermo-chemical properties of MgO-C refractories [14]. In recent years, magnesium aluminate ( $\text{MgAl}_2\text{O}_4$ ) spinel has been recognized as one of the most effective refractory material due to its excellent wear and penetration resistance towards slag and also resistance to change in operating environment [15-18]. Presence of micron sized  $\text{MgAl}_2\text{O}_4$  spinel as well as in-situ spinel (formation took place in the matrix by the direct reaction of magnesia and alumina) in the matrix of MgO-C refractories improves the thermal shock resistance and corrosion behavior of refractory products [18]. Presence of nano (size < 100nm) particles in MgO-C refractories have also improved the durability, thermal shock resistance, corrosion resistance and oxidation resistance [19-21]. Thus it is interesting to study the physical and chemical properties of MgO-C bricks with the addition of micron-sized and nano-sized  $\text{MgAl}_2\text{O}_4$  spinel.

Hence, in this chapter, a general introduction to MgO-C refractories and its application in ladles, role of spinel in MgO-C refractory and role of nanoparticles in refractory industries are described based on literature. The organization of thesis is given in the last part of this chapter. The main objectives of the present research work are presented at the end of the second chapter, which is based on a critical literature survey.

## 1.2 MgO-C refractory and its application in ladle

Refractories used for ladle lining must be able to withstand the increasing severity of service conditions associated with secondary steel making in order to produce various grades of steel with stringent specifications. The conditions during the steel refining processes are aggressive, which makes the refractory materials used in steel teeming ladles susceptible to a high degree of corrosion. In addition to corrosion, the brittle nature of refractory materials gives limitation to their applicability. Fig 1.1 shows the schematic view and various parts of the steel ladle. The different working lining designs of the steel ladle are given in Table 1.1.

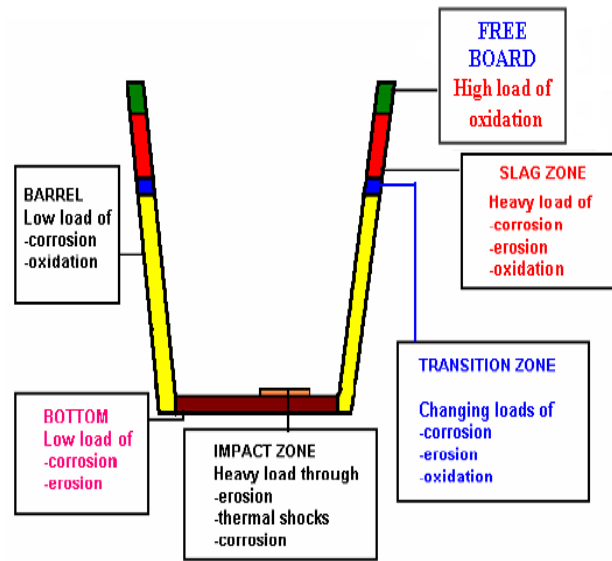


Fig.1.1: Schematic view and various parts of steel ladle

Table 1.1: Different working lining designs in steel ladles in India

Area	Bottom	Metal Zone	Slag Zone	Free Board
Refractory bricks used	MgO-C	MgO-C	MgO-C	MgO-C
	Al <sub>2</sub> O <sub>3</sub> -MgO-C	Dolomite	70% Al <sub>2</sub> O <sub>3</sub>	70% Al <sub>2</sub> O <sub>3</sub>
	70% Al <sub>2</sub> O <sub>3</sub>	Al <sub>2</sub> O <sub>3</sub> -MgO-C	80% Al <sub>2</sub> O <sub>3</sub>	80% Al <sub>2</sub> O <sub>3</sub>
	80% Al <sub>2</sub> O <sub>3</sub>	70% Al <sub>2</sub> O <sub>3</sub>	MgO-Cr <sub>2</sub> O <sub>3</sub>	Cr <sub>2</sub> O <sub>3</sub> -MgO
	MgO-Cr <sub>2</sub> O <sub>3</sub>	80% Al <sub>2</sub> O <sub>3</sub>		
		Cr <sub>2</sub> O <sub>3</sub> -MgO		

Some of the important properties requirements of refractories used in steel ladle are:

- High corrosion resistance to steel slag
- High abrasion resistance by liquid metal
- High thermal spalling resistance
- High hot strength and
- Low molten steel penetration

For the past several years, refractories based on MgO and C had performed tremendously well in many applications such as basic oxygen furnace (BOF), electric arc furnace (EAF), varieties of vessels and ladles for secondary refining treatments as compared to bricks without carbon due to high thermal conductivity, low thermal expansion, chemical inertness to slag and high thermal shock resistance [1-2].

MgO-C refractory, which is one of the highest consumable refractory item in steel sector with a specific consumption as high as 3.0 kg/ton in BOF and 2.5 kg/ton in EAF for the best shop's practice is the top most concern for any steel manufacturer. MgO-C refractories are unfired refractory, which is manufactured by mixing refractory grains, graphite and other additives with liquid resin and pitch as a binder and uniaxially pressed using a hydraulic press with a specific pressure of 2 T/cm<sup>2</sup>. The pressed bricks were tempered at 220-240 °C, to facilitate polymerization of resin into carbon and to eliminate residual water and phenols, there by developing sufficient strength [22]. The physical, thermo-mechanical and thermo-chemical properties of MgO-C refractories have improved significantly by selecting the right raw materials with respect to purity, grain size of MgO, binders, bonding systems and additives in both micron and nano range [5, 11, 12, 22, 23].

### **1.3 Role of spinel in MgO-C refractory**

The spinel minerals have the generic formula AB<sub>2</sub>O<sub>4</sub>, where 'A' is a divalent ions such as Mg<sup>2+</sup>, Fe<sup>2+</sup>, Mn<sup>2+</sup>, Zn<sup>2+</sup> and 'B' is a trivalent ions such as Al<sup>3+</sup>, Fe<sup>3+</sup>. The structure of spinels was described as having an oxygen ion sub lattice arranged in a cubic close-packed arrangement with cations occupying various combinations of the octahedral (O) and tetrahedral (T) sites. The cubic unit cell is large, comprising 8 formula units and containing 32 O and 64 T sites. Spinels are divided into two categories such as normal

and inverse spinel. In normal spinel, the divalent cations 'A' are located on the tetrahedral (T) sites and the trivalent cations 'B' on the octahedral (O) sites. In inverse spinels, the A cations and one-half the B cations occupy the O sites, with the remaining B cations occupying the T sites [24].

MgAl<sub>2</sub>O<sub>4</sub> spinel ceramic is of significant technological interest for refractory and structural applications at elevated temperature because spinel (MgAl<sub>2</sub>O<sub>4</sub>) is a refractory material, where no liquid formation takes place with any mixture of pure magnesia and alumina at temperature below 1900 °C. It has also high melting point, good mechanical strength and excellent chemical resistance. The major application areas of spinel refractories are transition and burning zones of cement rotary kilns, sidewalls and bottom of steel teeming ladles and checker work of glass tank furnace generators because they are resistant to corrosion by slag [25-29]. For such applications, spinel is used as a major component in an alumina rich or magnesia rich matrix, depending upon the environmental condition prevailing in the application zone. Hence, stoichiometric, magnesia rich and alumina rich spinel (non-stoichiometric) compositions are important from the application point of view.

Spinel always have a tendency for forming substitutional solid solution when comes in contact with slag due to its defective structure [30]. A complex nature of spinel such as (Mg, Mn, Fe)O·(Fe, Al)<sub>2</sub>O<sub>3</sub> was formed when Fe<sup>2+</sup> and Mn<sup>2+</sup> of the slag goes into A-site of spinel. Also Ca<sup>2+</sup> of slag reacts with excess Al<sub>2</sub>O<sub>3</sub> of spinel forming Hibonite (CA<sub>6</sub>) leading to densification of texture [30, 31]. Depletion of MnO, FeO and CaO makes the slag more viscous (due to increase of the relative amount of SiO<sub>2</sub>), which limits slag penetration and thereby reduces slag corrosion [32].

#### **1.4 Role of ceramic nanoparticles in refractory industry**

The refractory industry is highly matured and in order to counteract the stiff competition from foreign market, the only way is to develop new technologies that have high added value and cannot be easily copied. Thus the use of nanoparticles has brought about a revolution in refractories field by exhibiting remarkable performance [19-21]. Nanoparticles are nothing but ultrafine particles of size < 100 nm. When the grain size of the material reduces to nano scale, the relative volume of atoms in the grain boundary

enhances and the ordered arrangement conditions of original atoms or molecules will be destroyed leading to alteration of many properties such as structural, microstructural, chemical and mechanical [33, 34]. A small amount of nanoparticle addition in refractories has a great influence on its thermo-chemical properties. Nanoparticles disperse among spaces between coarse, medium and fine particles of refractory raw materials thereby filling of interior pores and gaps and improve the microstructure and reactivity [21]. Nano materials not only absorb and relieve the stress due to thermal expansion and shrinkage of refractory particles but also reduce the maldistribution of thermal stress in the inner portion of refractories [21]. Incorporation of nano materials also increases the strength and corrosion resistance of refractory at high temperature due to its high surface to volume ratio [21].

Addition of small amounts (~ 2 wt %) of nano-zirconia ( $\text{ZrO}_2$ ) in dolomite refractories resulted in the improvement of densification, thermal shock resistance, slaking resistance and slag corrosion resistance [35]. Presence of nano iron oxide in  $\text{MgO-Cr}_2\text{O}_3$  refractories facilitated the formation of magnesio ferrite spinel at lower temperatures which improves the physical and chemical properties of the bricks [36]. Addition of 0.4 wt% nano  $\text{Fe}_2\text{O}_3$  in silica refractories has improved the physical and chemical properties [37].

The castables used in iron and slag runners in blast furnace possesses superior slag corrosion resistance, excellent thermal shock resistance and mechanical properties due to the formation of nano-sized SiC whiskers (additives present in the matrix such as Si and  $\text{FeSi}_2$  results in formation of nano sized SiC whiskers at 1400 °C) [38]. A developed technique to study the hydration of castables was based on measuring the electrical conductivity. Addition of nano-sized poly carboxylate-ether based deflocculants lowers the electrical conductivity of the matrix suspension to values near 0.71 ms/cm there by facilitating achievement of self flowabilty of the castable [39]. Addition of nano  $\text{MgAl}_2\text{O}_4$  gel in castable system has resulted in tremendous improvement in thermal shock and corrosion resistance as compared to micron sized spinel addition [40-42].



## 1.5 Organization of the thesis

The addition of micron or nano ceramic in MgO-C refractories has significantly improved the thermo-chemical properties. Basic introduction of MgO-C refractories and its application in ladle along with the role of spinel and nano ceramics in refractories was discussed in chapter 1. Chapter 2 provides a detailed discussion of literature on different works on MgO-C refractories with respect to various types of raw materials, additives and binders. It also deals with literature review on synthesis of nano crystalline spinel through various non-conventional routes. It also covers the effect of physical and chemical properties of MgO-C refractory with the addition of nano materials. The main objective of the present work, which is based on the literature survey, is presented towards the end of chapter 2. Chapter 3 deals with the raw materials and refractory fabrication along with synthesis of nano-sized spinel using citrate-nitrate route. The characterization techniques used in the present work are described in detail in this chapter. Chapter 4 deals with the study of physical and chemical properties of micron-sized spinel addition in MgO-C refractories with respect to type and amount; characterization of nano  $\text{MgAl}_2\text{O}_4$  spinel powders synthesized using citrate-nitrate route and the effect of nano  $\text{MgAl}_2\text{O}_4$  spinel addition on the physical and chemical properties of MgO-C refractories. Finally, conclusions and scope for the future work are given in Chapter 5.

## **Chapter 2**

### *LITERATURE REVIEW*

## 2.1 Technological evolution of MgO-C refractories

Since 1950's, carbon has been recognized as an essential component of refractories. It was found that the addition of carbon leads to better thermal and chemical resistance, thereby increasing the life of refractory linings and indirectly reducing steel production cost [43, 44]. Carbon is now an integral component of the ceramic-carbon composite for many refractory applications. State-of-the-art, magnesia-carbon brick is the accepted standard for lining BOF and electric steelmaking furnaces and for the slag lines of ladle metallurgy furnaces [45]. The detail technological evolution of MgO-C refractories and its application area is given in Table 2.1.

Table 2.1: Technological evolution of MgO-C refractory [46, 47]

Year	Technology Evaluation
1950	<ul style="list-style-type: none"> <li>• Evolution and use of magnesia carbon and pitch bonded dolomite refractories; carbonisation carried out during preheat treatment of ladle; inhibiting slag penetration and thermal spalling.</li> <li>• Used in BOF.</li> </ul>
1970	<ul style="list-style-type: none"> <li>• Magnesia purity became a factor. Thus MgO grain with low boron and lime to silica ratio of 2 to 3:1 was used extensively to improve corrosion resistance.</li> <li>• Burned and impregnated magnesia brick with finite pore size to inhibit slag penetration and thermal spalling</li> <li>• Used in charge pad and other high wear areas in BOF.</li> <li>• Beginning of zonal lining concept.</li> </ul>
1980	<ul style="list-style-type: none"> <li>• Development of resin bonded magnesia-graphite refractories with higher carbon content.</li> <li>• Addition of antioxidants to preserve the carbon content.</li> </ul>
2000 – Till date	<ul style="list-style-type: none"> <li>• Use of high purity magnesia grains (fused / sintered) having large crystal size to further improves the corrosion resistance.</li> <li>• Variation of carbon content with respect to type and amount to improve the thermal conductivity and oxidation resistance.</li> <li>• Addition of various additives (such as metallic, alloy and inorganic compounds) to achieve improved hot strength, oxidation resistance and corrosion resistance.</li> <li>• In-situ spinel bonding to improve thermal spalling.</li> <li>• Use of nano additives.</li> </ul>

In spite of several efforts made to improve the performance of MgO-C bricks, the problems still exist due to increasing severity of operating condition by many folds. This has opened up the path for further research in this field. This is how use of spinel in refractories has come up in a broad way. Inconsistency in performance due to inhomogeneous microstructure has led several researchers to think for some alternative methods to achieve the desired properties and a consistent performance which has led to explore the possibility to incorporate nano additive in the matrix [19, 48]. The selection of base raw material greatly influences the properties and performance of refractories and was discussed in detail.

## **2.2 Selection of raw materials**

The main problems faced in steel ladle refractories are corrosion by steel slags, abrasion by liquid metal, thermal spalling, oxidation of carbon layer, deterioration of strength at high temperature and molten steel penetration [49-51]. The performance of refractories greatly depends on the selection of raw materials. Several studies had been carried out to find out the effect of different raw materials based on purity, porosity and crystallite size [52-54]. The raw materials include magnesia, graphite, resin and antioxidants. Selections of individual raw materials are described in detail.

### **(a) Magnesia**

Three different types of magnesia grains are used for the production of MgO-C bricks such as - sintered magnesia produced from natural magnesite; seawater magnesia produced by firing magnesium hydroxide extracted from seawater and fused magnesia produced by fusing sintered magnesia in an electric furnace [55, 56].

Several researchers reported the effects of magnesia aggregate on the corrosion resistance of MgO-C bricks. It was indicated that the magnesia aggregate with following characteristics, which led to superior corrosion resistance.

- (i) High concentration of fused magnesia rather than sintered magnesia [53, 57].
- (ii) Small content of  $B_2O_3$  and high ratio of  $CaO/SiO_2$  [58-60].
- (iii) Large periclase crystal grain [58]

The typical chemical and physical properties of magnesia aggregate are given in Table 2.2.

Table. 2.2: Chemical and physical properties of magnesia aggregate [58, 59].

Properties		Products					
		Seawater		Natural		Brine	
		Fused	Sintered	Fused	Sintered	Sintered	Sintered
Chemical composition (%)	MgO	99.07	99.13	96.55	98.32	95.46	99.30
	SiO <sub>2</sub>	0.20	0.22	1.29	0.57	1.96	0.02
	Al <sub>2</sub> O <sub>3</sub>	0.06	0.06	0.12	0.08	0.90	0.05
	Fe <sub>2</sub> O <sub>3</sub>	0.11	0.04	0.75	0.44	0.67	0.01
	CaO	0.57	0.51	1.19	0.58	0.98	0.67
	B <sub>2</sub> O <sub>3</sub>	0.02	0.04	Traces	Traces	Traces	Traces
Apparent porosity (%)		2.60	1.50	1.10	0.80	8.0	2.0
Bulk specific gravity		3.46	3.40	3.54	3.55	3.20	3.43
Periclase grain (μm)		>200	20-40	>50	>100	20-60	20-40

#### (b) Graphite

Carbon in the form of natural-flake graphite made up of well-formed crystals was often used in MgO-C brick. Characteristics of flake graphite are given in Table 2.3.

Table 2.3: Characteristics of flake graphite used for carbon containing refractories [13, 61]

Characteristics	China		India	Source	
	1	2		Malaysia	Japan
Grain size distribution (wt-%)					
> 0.5 mm	13.2	0.9	2.6	12.5	-
0.50 - 0.297 mm	35.0	8.8	28.2	27.3	-
0.297 - 0.177 mm	26.4	49.1	65.6	40.6	6.8
0.177 - 0.125 mm	11.4	38.3	3.0	13.2	12.7
0.125 - 0.063 mm	8.9	2.4	0.4	5.2	42.5
< 0.063 mm	5.0	0.4	0.2	1.2	38.0
Avg. grain size (mm)	0.286	0.194	0.262	0.276	0.075
Ash content (%)	14.5	6.0	12.6	11.8	13.7
Minerals in ash:					
Quartz	+	+	+++	+	++
Mica (Biotite)	+	+	++	+++	-
Kaolinite	+	+	+	++	+
Chlorite	+	-	-	-	+
Feldspar	-	+	+	-	+
Vermiculite	+	+	+	+	+
+++ <i>Very strong</i> ++ <i>Strong</i> + <i>Weak</i> - <i>Very weak</i>					

Presence of minerals like quartz, kaolinite and anorthite in ash of graphite possesses an adverse effect on the corrosion resistance of MgO-C brick. Impurities in ash of flake graphite after decomposition reacts with MgO grains to form low melting phases, thereby decreases the corrosion resistance [62]. Hence, carbon purity should be kept as high as possible. The roles of graphite are (i) it fills the porous brick structure; (ii) hinders the slag penetration in to the brick due to high wetting angle between slag and graphite that leads to the formation of dense layer of MgO and CO at the slag-brick interface and (iii) improves the thermo-mechanical spalling (surface splitting of the lining) resistance of brick due to high thermal conductivity and low thermal expansion of graphite. The size of graphite also plays a vital role for improving the oxidation, abrasion and corrosion resistance of MgO-C bricks [63].

The major problem faced during manufacturing MgO-C brick is compressibility of graphite in the mixture to get a dense structure. Thus pressing of a dense brick greatly depends on the type of binder used.

### **(c) Resin**

Initially, pitch was used as binder for MgO-C brick. However, it was difficult to prepare a dense brick containing a large amount of flake graphite due to the elastic character of graphite, which causes the brick to expand during heat treatment leading to poor adhesion of graphite to the matrix. Hence resin was found to be the best binding agent for MgO-C refractories [64].

Phenolic resin is the most common binder used in carbon containing refractories due to the following excellent features.

- (i) Chemical affinity towards graphite and refractory aggregates
- (ii) High adhesive property leading to high handling strength.
- (iii) Being thermosetting in nature it imparts high dry strength.
- (iv) Strong carbon bonding was achieved due to high content of fixed carbon (52%).
- (v) Environmentally, it was less harmful than tar pitch.
- (vi) Superior kneading and pressing characteristics.
- (vii) Polymerization of resin (100-200°C) leads to isotropic interlocking structure.
- (viii) Higher resin content increases the cold crushing strength (CCS) and strength of the tempered bricks.

During winter, the viscosity of resol resin increases, which often causes low dispersion of ingredients in the mixer machine [65]. On the contrary, in summer, the viscosity of resin sometime causes the green body to weaken its stiffness, resulting in lamination of bricks [65]. In order to overcome the reduction in viscosity, powder novalac resin was added into resol resin [65].

Main demerit of carbon bearing material is the removal of carbon through oxidation at high temperature. This process makes the brick texture loose and prone to attack by slag thereby reducing the life of the refractory brick [66]. Thus to check the removal of carbon by oxidation, metallic addition was done in smaller amounts which was known as antioxidants.

#### **(d) Antioxidants**

The main drawback of carbon containing refractories was the oxidization of carbon. The oxidation of carbon took place in two different ways [67, 68]: direct oxidation and indirect oxidation. Below 1400 °C, direct oxidation occurs when carbon was oxidized directly by the oxygen from atmosphere. Above 1400 °C, indirect oxidation took place that leads to a partial loss of both Mg and C from the refractories. On prolonged exposure to temperature above 1500 °C, Mg vapor forms and simultaneously deoxidizes to MgO. A dense secondary oxide phase of MgO layer adjacent to the hot face of the refractories was formed, that causes an increase in oxidation resistance of the material during operation at high temperature. Thus to prevent oxidation of carbon, different antioxidants such as aluminium (Al), silicon (Si) and boron carbide ( $B_4C$ ) are used in MgO-C refractories [66, 68-72]. Al and Si antioxidants are mostly used due to their low cost and effective protection, which once formed remain stable as a discrete phase in the bulk of the specimen. The formation of  $Al_4C_3$  and SiC inhibits the oxidation of carbon [68].  $B_4C$  reacts with air to form liquid boron oxide, which adheres to the refractory surface as a protective layer thus preventing oxygen to come in contact with refractory material [69, 71]. Now-a-days, new generation of boron based antioxidants like  $ZrB_2$ ,  $CaB_2$ ,  $CaB_6$ ,  $Al_8B_4C_7$ , Mg-B,  $CrB_2$  and  $SiB_6$  have come to the market that react to form liquid phase, thereby filling the pores and preventing the oxidation of carbon [73-81].

### 2.3 Role of micron-sized, stoichiometric and in-situ spinel in MgO-C brick

In recent years,  $\text{MgAl}_2\text{O}_4$  spinel is of significant technological interest for refractory applications at elevated temperature as because it is an environment friendly material possessing and also a good combination of both physical and chemical properties [16, 82-86] such as:

- High-melting point
- High chemical inertness against both acidic and basic slags
- Low thermal expansion at elevated temperatures
- Resistance to slag corrosion
- High thermal shock resistance
- Excellent hot strength
- Low content of secondary oxide phases, providing good refractoriness
- High resistance to changes in the environment and
- Ecologically benign refractory material

$\text{MgAl}_2\text{O}_4$  spinel added MgO-C refractory has been improved continuously under ecological and economical aspects, mainly in terms of binders and additives used for better thermo-mechanical properties and reinforced oxidation resistance [27]. In addition to that,  $\text{MgAl}_2\text{O}_4$  spinel added MgO-C refractories exhibit unique mechanical, thermal and chemical properties. Therefore they are established as high duty refractory products in application of various parts of converters, slag zone of electric arc furnaces and ladles [25-27].

Various grades and sizes of  $\text{MgAl}_2\text{O}_4$  spinels are commercially available in the market with different alumina and magnesia contents. Depending upon the application condition, the type of spinel was chosen. MgO rich spinel addition in refractories is preferred for cement rotary kilns, whereas refractories containing  $\text{Al}_2\text{O}_3$  rich spinel are preferred for steel ladles [82, 83, 87, 88]. It was observed that high alumina castables with micron sized spinel addition have given superior performance in the sidewalls and bottom of steel ladles along with MgO-C bricks in slag line due to depletion of MnO, FeO and CaO in slag and the formation of  $\text{CA}_6$  which make the slag more viscous and less penetrative [89, 90]. Addition of micron-sized spinel in the refractories increases the slag corrosion resistance [90, 92].



It was reported that addition of stoichiometric spinel improves the slag erosion and penetration resistance due to the formation of gehlenite ( $C_2AS$ ),  $CA_2$  and  $CA_6$  phases at the hot face [15]. So, the relative amount of silica increases to generate a high viscous and high melting temperature slag which may be a probable cause for preventing further slag penetration resulting in improved slag resistance for spinel added high alumina castables [89].

The properties of refractory materials can also be enhanced by in-situ spinel formation in the site. The in-situ spinel formation starts around  $1000^{\circ}C$  and gets accomplished above  $1300^{\circ}C$  [17, 18]. It is accompanied with volume expansion which leads to a significant reduction in pore volume [16, 93-95]. The formed spinel particles are found almost in the periphery of the periclase grains and play a vital role in improving the refractory properties. Formed spinel minimizes the open pores and leads to densification of matrix thereby preventing slag penetration. In-situ spinel formation also improves the corrosion and thermal shock resistance [16, 17, 96, 97]

The amount of in-situ spinel formation was to be optimized to get sufficient tightening of the joints, which prevents the liquid metal penetration. Structural spalling resistance was increased due to the development of micro cracks [mismatch thermal expansion co-efficient between  $MgO$  ( $13.5 \times 10^{-6}/^{\circ}C$ ) and  $MgAl_2O_4$  ( $7.6 \times 10^{-6}/^{\circ}C$ ) grains] [16, 17]. On other hand, higher amount of spinel formation leads to higher expansion and thereby leading to development of stresses, which causes structural spalling and increased slag penetration [16, 17]. So, controlled spinel formation is always desirable.

## 2.4 Mechanisms of corrosion in MgO-C bricks

During refining of steel in ladle, corrosion of the lining material in contact with slag took place due to the following phenomena [90, 98, 99]. Fig. 2.1 shows the different phenomena of corrosion in refractories.

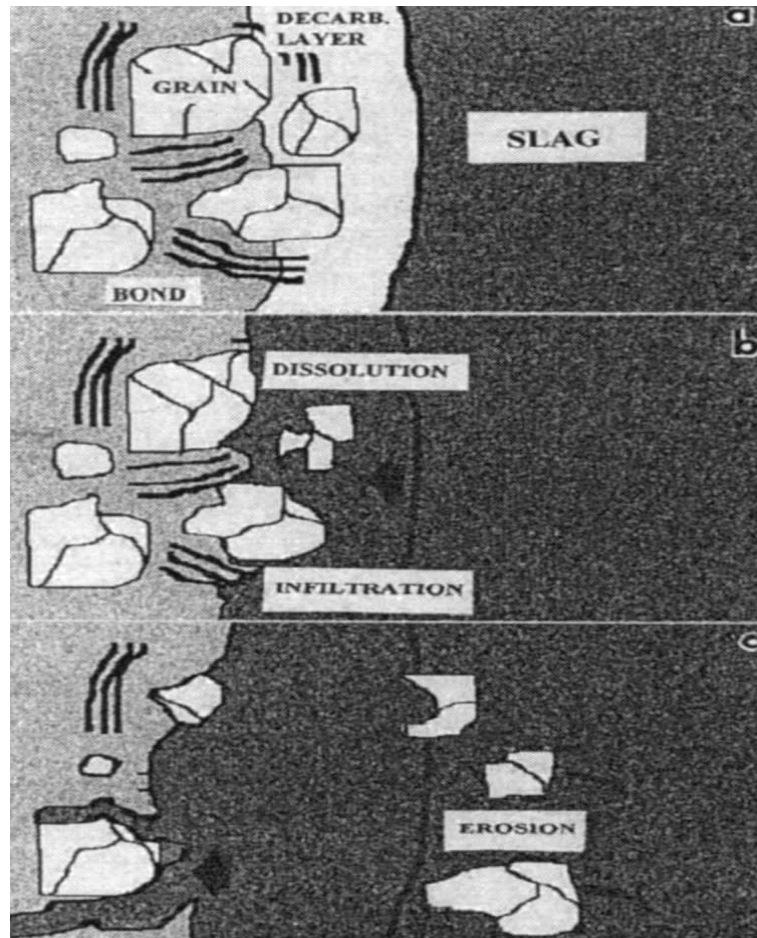


Fig. 2.1: Different phenomena of corrosion in refractories [Adapted from ref. 98, 99]

- (i) Dissolution is a chemical process by which the refractory material was continuously dissolved by the diffusion of reacting species through the liquid slag.
- (ii) Penetration is a process by which the slag penetrates into the pores that causes deterioration of the refractory wall due to differential expansion or contraction between refractory and the slag.

(iii) Erosion is the process of wear out of refractory material which depends on viscosity of slag and velocity of gases that comes in contact with the refractory material.

Corrosion of carbon containing refractories follows the following three stages simultaneously with the above phenomena [98-100] such as:

- (i) Formation of a decarburized layer that may be due to oxidation of graphite.
- (ii) Infiltration of slag into the decarburized layer and erosion of the oxide grain.
- (iii) Reduction of oxide grains at high temperature ( $\sim 1600^{\circ}\text{C}$ ) reaction with carbon those results in its exposure to slag and further erosion.

Diffusion of slag particles into refractory material causes a change in the physical properties. The higher wetting angle makes it more difficult for the slag to penetrate into pores and cracks in the refractory [101]. This was not the only thing that affects the infiltrating depth. The infiltrating depth was also affected by the temperature gradient in the brick [101]. The temperature gradients causes the viscosity of slag to increase with an increasing distance into the refractory (colder), thereby decreasing the infiltration depth will get decrease. Fig. 2.2 shows the penetration of slag in the refractory as it proceeds from hot face to cold face. The penetration depth depends on hot face temperature of refractories, slag temperature and its viscosity. Penetration increases with increase in hot face temperature, slag temperature and decrease in slag viscosity.

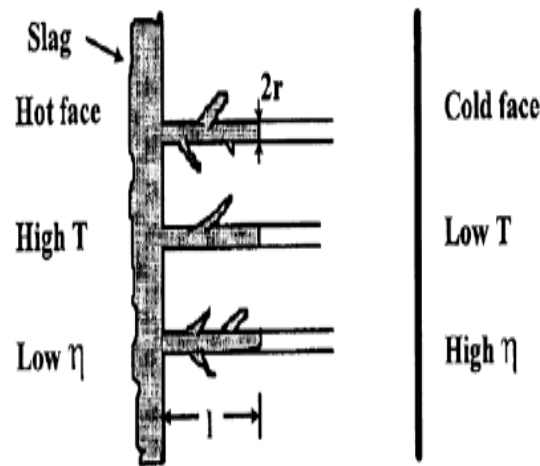


Fig. 2.2: Different penetration conditions of slag in refractory. [Adapted from ref. 98]

## 2.5 Effect of nanoparticles on the properties of MgO-C refractories

Nano technology has been introduced into refractories field in recent years in order to eliminate the problems related with their performance arising out of inhomogeneous microstructure. It has been apprehended that the performance of refractories could be appreciably improved by improving the thermo-chemical properties due to well dispersion of nano-sized particles in the matrix of the refractories [33, 34].

The refractory brick is made up of aggregate and matrix. The aggregate part is composed of particles of size ranging from several micrometers to millimeter. The matrix part is composed of particles of size less than or equal to 500  $\mu\text{m}$ . Around 25 vol % of the total brick structure was occupied by the matrix. Out of which 10 vol% comprises of pores. The physical and chemical properties of the refractories depend on the particle size, pore size as well as its distribution and gap between aggregate and matrix phase [19]. Thus nanoparticles can easily modify the microstructure as per the requirements by filling the gap and modifying the pore size distribution.

Use of nearly 5 vol % ( $\sim 1.5$  wt-%) nano carbon (two different types such as single sphere and aggregate) in MgO-C refractory has improved the thermal shock resistance, and bond strength [19]. The addition of single sphere type nano carbon has led to densification of matrix, thereby improving the erosion resistance. Aggregate type of nano carbon provides elasticity, which in turn decreases the stress relaxation and improves the thermal shock resistance. In addition to this, aggregate type nano carbon provides pore segmentalization and pore volume control (rich in micro pores), thereby leading to minimization of heat loss and avoiding shell deformation. However, the combination of both types of nano carbon in MgO-C refractory counter balances the thermal spalling resistance and corrosion resistance [19].

Use of low amount of nano carbon (2 vol %, 10 nm size) and higher amount of flake graphite (8%,  $\sim 0.3$  mm) in MgO-C refractories improves heat insulation and decreases the shell deformation and increases shell life of vessel [21]. It was also reported that the addition of 1.5% nano-particles showed better thermal spalling resistance as compared to that of refractories containing 18% graphite [20].

Titanium carbide is an excellent non oxide ceramics with high melting point, hardness and electrical conductivity with good wear resistance, corrosion resistance, thermal conductivity and good chemical stability. However, the use of titanium carbide in refractory industry was limited because of its high cost. Recently, Arasu et. al. [102] has investigated the formation of in-situ titanium carbide in the matrix of the MgO-C system by adding nano  $\text{TiO}_2$  that improves the physical and chemical properties of MgO-C bricks.

## **2.6 Synthesis of $\text{MgAl}_2\text{O}_4$ spinel using different chemical routes**

$\text{MgAl}_2\text{O}_4$  spinel is industrially produced either from magnesite and alumina or magnesite and bauxite by fusion or sintering. Spinel aggregate produced by fusion or sintering routes have relatively low reactivity. Different synthesis routes have been developed for producing  $\text{MgAl}_2\text{O}_4$  spinel [103-109]. Different additives were introduced for betterment of physical and chemical properties of  $\text{MgAl}_2\text{O}_4$  spinel produced which will be used in the refractory products [110-112]. It was very difficult to produce ultra fine, reactive spinel powders from the aggregates. For this reason, various wet chemical methods have been successfully developed for producing nano spinel powders [113, 114]. Table 2.4 shows the different processes implemented by various researchers using different processing conditions.

The precursor particles produced through different wet chemical routes tend to agglomerate during drying. Severely agglomerated spinel powders have difficulty in sintering, especially at relatively low temperatures. Therefore combustible ingredients are introduced into the precursors prepared by co precipitation to reduce the formation of hard agglomerates during drying and firing. Hence, in this work,  $\text{MgAl}_2\text{O}_4$  spinel nanopowders have been synthesized through citrate-nitrate route.

Table 2.4: Various routes for preparation of nano MgAl<sub>2</sub>O<sub>4</sub> spinel

Methods	Remarks	References
Citrate-nitrate	Citrate to nitrate ratio 1:1; MgAl <sub>2</sub> O <sub>4</sub> formation started at 650 °C and size was 30 – 50 nm.	[115, 116]
Co-melting	1:1 to 1:1.4 ratio of Al to Mg nitrates; crystallite size was 12-59 nm.	[117]
Co-precipitation	1:2 ratio of Mg and Al with sintering aid (ZnO or MnO <sub>2</sub> ). pH maintained between 9.5-10.5 Particle size was 25-60 nm.	[118]
Sol-gel	Metal alkoxides of Al(OC <sub>3</sub> H <sub>7</sub> ) <sub>3</sub> and Mg(OC <sub>2</sub> H <sub>5</sub> ) <sub>2</sub> were used. Surface area of amorphous powder is 260 m <sup>2</sup> /gm. Crystallite size was 30 nm.	[119]
Sol-gel citrate	Spinel (size around 20 nm) formation started at 400°C	[120]
Microwave assisted combustion	Use of modified domestic microwave oven Crystallite size of spinel synthesized using microwave and combustion synthesis was 20-50 nm and 100-250 nm, respectively	[121]
Freeze drying	Production of fine homogeneous particles. Particle size of spinel powder after calcined at 1100°C/12 h is about 50 nm.	[122]
Flame spray pyrolysis	Resultant spinel powder was spherical, dense and homogeneous. Specific surface area is 40-60 m <sup>2</sup> /g. Average particle size is 25-45 nm.	[123]

## 2.7 Summary of literature

The extensive literature survey reveals that in spite of several research regarding the improvement of life and performance of MgO-C refractories with respect to different types of raw materials (type, crystalline size and purity), binders (type and viscosity) and additives (carbon, antioxidants and special oxides), still there is a scope of further improvement on the properties and performance of MgO-C refractories due to increase in severity of operating condition, greater demand for production of cleaner steel and low specific consumption of refractory in steel sector.

MgO-C bricks were used in slag line of ladles due to superior slag penetration resistance and excellent thermal shock resistance. The life of this refractory has limited on prolonged use and increasing severity of operating conditions due to poor oxidation resistance and low strength at high temperatures. It was observed from the literature that, addition of  $\text{MgAl}_2\text{O}_4$  spinel (either in micron, or stoichiometric or in-situ) exhibits unique mechanical, thermal and chemical properties of refractories.

The particle size of spinel is also an important factor that influences both physical and chemical properties of refractories. Addition of nanoparticles in different refractory systems has resulted in tremendous improvement in thermo-mechanical as well as thermo-chemical properties. A very few literatures are available on the effect of the physical and chemical properties of MgO-C bricks with addition of micron-sized and nano-sized  $\text{MgAl}_2\text{O}_4$  spinel. Thus, there is further scope to improve the thermo-mechanical as well as thermo-chemical properties of MgO-C refractories with addition of micron-sized (type and amount) and nano-sized  $\text{MgAl}_2\text{O}_4$  spinel.

## **2.8 Objectives of the present studies**

The main objective of the present work:

To improve the physical and chemical properties of MgO-C refractories with the addition of  $\text{MgAl}_2\text{O}_4$  spinel in micron (with respect to type and amount) and nano range.

In this work, a set of experiments was carried out in order to standardize the type and amount of preformed spinel addition in MgO-C refractory system. Here, micron-sized spinel in three different commercially available grades [near stoichiometric (AR-78), alumina rich (AR-90) and magnesia rich (MR-66)] were used.

The standardized type and amount of spinel (10 wt % AR-78) was taken in order to compare and carry out the second set of experiments. In this experiment, the effect of without, standardized micron-sized (10 wt % AR78) and nano-sized  $\text{MgAl}_2\text{O}_4$  spinel added MgO-C bricks are correlated.

The spinel nanopowders were prepared by citrate-nitrate route, which is known to result in the production of nanocrystalline materials and these nanopowders (calcined at 800 °C) were used during fabrication of nano spinel added MgO-C brick.

## Chapter 3

### *EXPERIMENTAL WORK*

This chapter covers three sections. The first section covers the properties of different types of raw materials used for the fabrication of micron and nano-sized spinel added MgO-C brick. Second section covers the synthesis procedure for the preparation of nano-sized  $\text{MgAl}_2\text{O}_4$  spinel and third section describes the different characterization technique to study the different properties of micron-sized and nano-sized  $\text{MgAl}_2\text{O}_4$  added MgO-C bricks.



### 3.1 Raw materials and fabrication of micron and nano spinel added MgO-C brick

Commercially available high quality fused magnesia (FM), natural flakes graphite, aluminium metal powder ( $-150\text{ }\mu\text{m}$ ), three different types of micron sized spinel such as AR-78, AR-90 and MR-66 with two different grading ( $-45\text{ }\mu\text{m}$  up to  $10\text{ wt-}\%$  and  $0.5 - 1.0\text{ mm}$  for  $15\text{ wt-}\%$  to  $25\text{ wt-}\%$ ) to maintain granulometry of the mixture. Liquid resin and other additives were also taken as base raw materials for fabrication of micron sized spinel added MgO-C bricks.

In this present work, FM97LC was selected as a raw material for fused magnesia in order to get the purest MgO, best CaO/SiO<sub>2</sub> ratio, lowest possible Fe<sub>2</sub>O<sub>3</sub> content, highest specific gravity and large crystals in the range of  $500 - 1500\text{ }\mu\text{m}$  having less number of grain boundaries [58, 59, 124]. The physical and chemical analysis of flake graphite is given in Table 3.1 and the physical and chemical analysis of liquid resin and pitch powder is given in Table 3.2.

Table 3.1: Physical and chemical analysis of flake graphite

Raw materials	Carbon (%)	Volatile matter (%)	Ash (%)	Surface area ( $\text{m}^2\text{g}^{-1}$ )
Flake graphite	94.1	1	5.3	1

Table 3.2: Physical and chemical analysis of liquid resin and pitch powder

<b>Property</b>	Liquid Resin	Pitch Powder
Viscosity (cps)	8500 - 9000	-
Specific gravity	1.23	-
Non-volatile matter (%)	80.10	-
Fixed carbon (%)	47.85	52
Moisture (%)	$\sim 4.0$	-
Volatile matter (%)	-	47
Ash (%)	-	1.4
Softening point ( $^{\circ}\text{C}$ )	-	135

The chemical composition of fused magnesia and three different types of spinel is given in Table 3.3.

Table 3.3: Chemical composition in percentage of fused magnesia and spinel

Raw Materials	Chemical composition					
	MgO	Al <sub>2</sub> O <sub>3</sub>	SiO <sub>2</sub>	CaO	Fe <sub>2</sub> O <sub>3</sub>	Na <sub>2</sub> O
Fused magnesia	97.34	0.08	0.40	1.40	0.50	0.50
AR-78	23.00	76.00	0.06	0.30	0.10	0.15
AR-90	9.00	90.00	0.05	0.25	0.10	0.17
MR-66	33.00	66.00	0.09	0.40	0.10	0.05

MgO-C bricks with sixteen compositions have been fabricated using different raw materials by varying micron sized spinel type and content starting from 0 to 25 wt % with an incremental addition of 5 wt % in MgO-C refractories. In this work, 0 wt% corresponds to without spinel added MgO-C brick and was denoted as ‘ZS’. The batch composition (total 16 numbers) of MgO-C brick with micron sized spinel is given in Table 3.4.

Table 3.4: Batch composition of micron sized spinel added MgO-C bricks

Raw materials	Weight percentage					
FM 97%LC	86.5	81.5	76.5	71.5	66.5	61.5
Graphite	12.5	12.5	12.5	12.5	12.5	12.5
AR-78 / AR-90 / MR-66	0	5	10	15	20	25
Al- metal powder	1	1	1	1	1	1
Resin liquid	3	3	3	3	3	3
Pitch powder	1	1	1	1	1	1

Nano spinel has been prepared using citrate-nitrate method (discussed in section 3.2). The as-synthesized spinel was calcined at 800 °C to get a pure  $\text{MgAl}_2\text{O}_4$  spinel. The calcined spinel nanopowders in different weight percentage such as 0.1, 0.5, 1 and 1.5 were used in MgO-C bricks. In this work, nano-spinel addition in MgO-C brick was denoted as ‘NS’. The batch composition of nano spinel added MgO-C brick is given in Table 3.5.

Table 3.5: Batch composition of nano spinel added MgO-C refractory

Raw materials	Weight percentage					
FM 97%LC	86.5	76.5	86.5	86.5	86.5	86.5
Graphite	12.5	12.5	12.5	12.5	12.5	12.5
AR-78	-	10	-	-	-	-
NS	-	-	0.1	0.5	1.0	1.5
Al- metal powder	1	1	1	1	1	1
Resin liquid	3	3	3	3	3	3
Pitch powder	1	1	1	1	1	1

All the raw materials were properly mixed thoroughly using high intensive mixer machine at room temperature for nearly 40 minutes. Table 3.6 shows the mixing sequence of various raw materials.

Table 3.6: Mixing sequence of MgO-C bricks

Steps	Mixing Sequence	Mixing Time (Min)
1	Coarse + Graphite + Aluminum metal powder + Hard pitch powder	2
2	Addition of liquid resin	15
3	Addition of dust fractions	20
4	Addition of resin powder	2
Total mixing time		~40

After mixing, micron sized spinel added bricks were pressed with a specific pressure of 2 Ton / cm<sup>2</sup> using hydraulic press (SACMI, Italy). Nano spinel added bricks were pressed into cylinder of dimension 50 mm x 50 mm using laboratory uniaxial press (1.8 Ton/cm<sup>2</sup>) rather than industrial press due to the non-availability of bulk amount of synthesized spinel. Lot of difficulties were faced during mixing and pressing such as improper dispersion while mixing and lamination as well as crack formation during pressing for 1.5 wt % nano spinel addition. The pressed samples were tempered at 220-250°C in a tempering kiln. Coking was carried out at 1000°C for 4 h under reducing atmosphere (carbon bed). The physical and chemical properties of the micron as well as nano-sized spinel added MgO-C bricks were characterized using different instrumental techniques (discussed in section 3.3).

### 3.2 Synthesis of MgAl<sub>2</sub>O<sub>4</sub> spinel nanopowders

Nanopowders of MgAl<sub>2</sub>O<sub>4</sub> spinel were prepared using citrate-nitrate method. Fig. 3.1 shows the schematic flow diagram for the synthesis of nano MgAl<sub>2</sub>O<sub>4</sub> spinel through citrate-nitrate method.

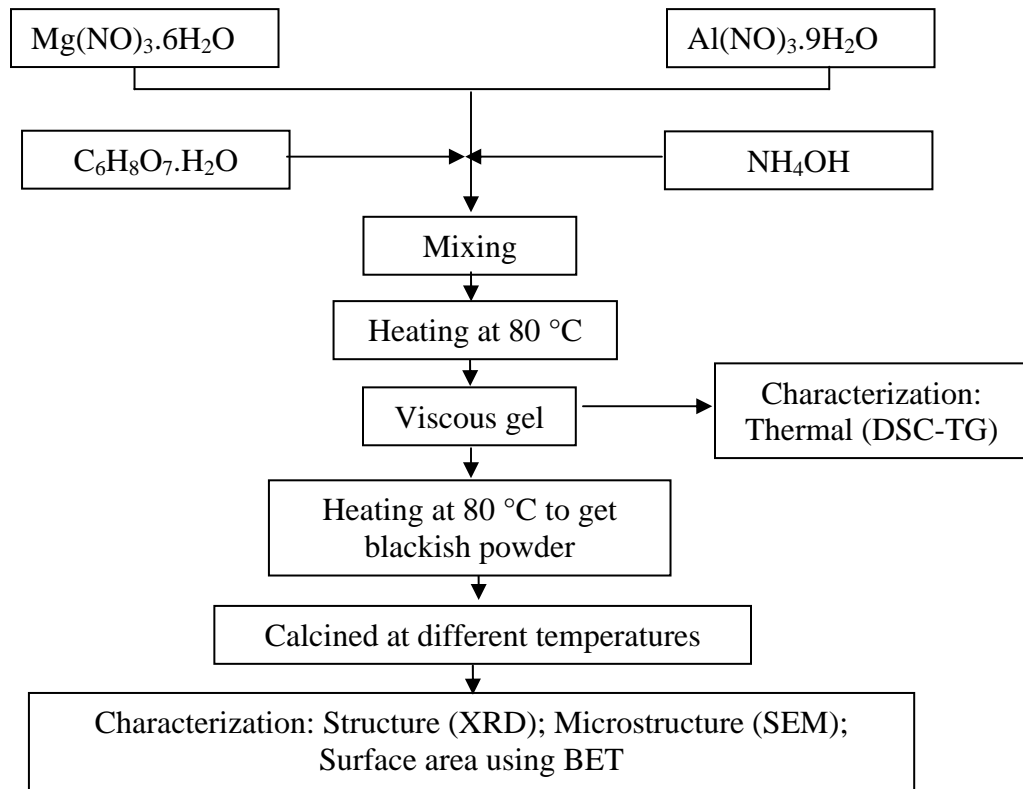


Fig. 3.1: Schematic flow diagram for the preparation of MgAl<sub>2</sub>O<sub>4</sub> spinel nanopowder

Reactants used for preparation of nano-sized  $\text{MgAl}_2\text{O}_4$  spinel were magnesium nitrate  $[\text{Mg}(\text{NO}_3)_2 \cdot 6\text{H}_2\text{O}]$ , aluminium nitrate  $[\text{Al}(\text{NO}_3)_3 \cdot 9\text{H}_2\text{O}]$ , citric acid  $[\text{C}_6\text{H}_8\text{O}_7 \cdot \text{H}_2\text{O}]$  and ammonia ( $\text{NH}_4\text{OH}$ ) solution. All chemicals were used as-received. A stoichiometric amount of magnesium nitrate, aluminium nitrate and citric acid were dissolved in distilled water. The metal to citrate ratio was maintained at 1:1. The solutions were mixed thoroughly and slowly evaporated on a heater. The temperature was maintained at 80 °C. A highly viscous gel was heated at 80 °C for 2h to get blackish powder. The fine powders were collected and calcined at different temperatures starting from 600 °C to 800 °C. The gel and calcined powders were characterized using different instrumental techniques (described in section 3.3).

### 3.3 General characterization

#### 3.3.1 AP, BD and CCS

Apparent porosity (AP), bulk density (BD) and cold crushing strength (CCS) were measured as per the standard of IS: 1528, Part-8 (1974), IS: 1528, Part-12 (1974) and IS: 1528, Part-4 (1974) respectively for both tempered and coked samples. Each value of AP, BD and CCS was of average of five parallel samples.

#### 3.3.2 HMOR

Hot modulus of rupture (HMOR) was determined by the conventional three-point bending test conforming to ASTM C133-97 [125], using HMOR testing apparatus (Netzsch 422, Germany). All the specimens for HMOR testing are dried at 110°C after wet cutting, without pre-firing in air atmosphere. The heating rate for HMOR testing was 5°C/min and the final firing temperature is 1400°C in air atmosphere with a soaking time of 30 min. The loading rate for HMOR was 0.15 MPa/sec.

The HMOR value was calculated by the following formula:

$$\text{HMOR} = (3W \times L) / (2b \times d^2) \quad 3.1$$

where “L” is the span length between the lower supporting points (12 cm for all the tests in this work); “W” is the maximum load when the specimen is broken (kg); “b” is the breadth (cm) and “h” is the height of the specimen (cm). Each value of HMOR was the average of five parallel specimens.

### 3.3.3 MOE

Modulus of elasticity (MOE) test was conducted by using non-destructive ultrasonic test at room temperature and it was measured indirectly by measuring the sonic velocity within the brick by passing ultrasonic signal through it. This test is of prime importance in assessing the spalling resistance of the MgO-C refractory bricks. For this test, the trial samples were cut into 25×25×150 mm and dried into 110°C for 3 h before testing. The ultrasonic waves were passed into the sample from one end to another end and time traveled was calculated.

The MOE value was calculated by the following formula:

$$\text{MOE} = (d \times v^2 \times s) \quad 3.2$$

where “d” is the bulk density of test sample (g/cc), “v” is the length (l) of the test specimen / time (t) travels (μ.sec) for the ultrasonic waves were passed into the sample from one end to another end and “s” is the poisson’s ratio (0.90 for magnesia-carbon sample).

### 3.3.4 TSI

Thermal spalling index (TSI) is the ratio between the modulus of rupture (HMOR) and the modulus of elasticity (MOE). The HMOR/MOE ratio was adopted as a simple index to evaluate the thermal spalling resistance.

### 3.3.5 Oxidation resistance

For oxidation resistance test, cylindrical samples (height = 50 mm, diameter = 50 mm) were cut from the tempered bricks and placed in an electrically heated furnace (heating rate of 5°C/min) under ambient condition at 1200°C for 5 h. The furnace is then cooled down at the rate of 5°C/min. After cooling, the samples were horizontally cut into two pieces. After oxidation test, the black surface remaining was measured at eight different locations and the average value was noted down.

### 3.3.6 Rotary slag corrosion test for micron sized spinel added MgO-C bricks

A dynamic slag corrosion test was conducted using rotary furnace (shown in Fig. 3.2) for micron-sized spinel added MgO-C bricks. Corrosion resistance of the samples was studied by using a conventional gas-fired rotary slag test furnace charged with steel making ladle slag. Its chemical composition and basicity are given in Table. 3.7. The corrosion test was carried out at 1650°C in air for 2 h. The reacted slag was refreshed every 30 min by charging 300 g of new slag to ensure constant slag composition during the test. After the slag corrosion test, the furnace was cooled naturally to room temperature. The sections after slag attack are visually compared and corrosion in millimeter was calculated by measuring the corroded area of the bricks.

Table 3.7: Chemical composition (%) and basicity of the steel making ladle slag

CaO	SiO <sub>2</sub>	Al <sub>2</sub> O <sub>3</sub>	MgO	Fe	MnO	CaO/SiO <sub>2</sub>
53.36	12.94	24.80	5.48	0.81	0.51	4.12



Fig.3.2: Rotary furnace for conducting slag corrosion test for micron-sized spinel added MgO-C bricks

### **3.3.7 Static crucible slag corrosion test for nano sized spinel added MgO-C bricks**

Slag corrosion test by static crucible test method was carried out for nano spinel added MgO-C sample at 1650°C for 2 h with steel making ladle slag. Chemical composition (%) and basicity of the steel making ladle slag are given in Table 3.7. The sections after slag attack are visually compared and corrosion in millimeter was calculated by measuring the corroded area of samples.

### **3.3.8 Pore size distribution**

The test samples (cube shape of  $10 \times 10 \times 10 \text{ mm}^3$  was cut from the tempered bricks) were dried at 110°C for 4 h and cooled in desiccator. The test samples were placed in pycnometer which was inserted in the part of the mercury porosimetric sample holder machine with a vacuum of 50  $\mu\text{m Hg}$ . Mercury porosimeter has been used to test the samples with a maximum pressure of 33000 psi. Surface tension and contact angle of mercury was 485 dynes/cm<sup>2</sup> and 130° respectively. Pore size distribution pattern i.e. open pore volume available for 'Hg' intrusion under pressure with respect to pore diameter has been characterized.

### **3.3.9 Thermal**

Differential scanning calorimetry (DSC) and thermal gravimetry (TG) of the gel (which was formed during synthesis of nano spinel using citrate-nitrate method) was carried out on thermal analyzer (Netzsch, Germany) with a heating rate of 10° C / min in argon atmosphere.

### **3.3.10 Surface area**

Surface area of the nano  $\text{MgAl}_2\text{O}_4$  powder was determined using Brunauer-Emmett-Teller (BET) surface area [Quantachrome, USA]. The measured surface area was converted to equivalent particle size according to the equation:  $\text{Size}_{\text{from BET}} = [6000 / (\text{density} \times \text{surface area})]$ . The density of  $\text{MgAl}_2\text{O}_4$  was taken as 3.28 g/cc.



### **3.3.11 Phase analysis**

Phase analysis of nano  $\text{MgAl}_2\text{O}_4$  powder was carried out by X-ray diffraction pattern (XRD, PANanalytical, Netherland) using  $\text{Cu-K}\alpha$  ( $\lambda=1.542 \text{ \AA}$ ). The crystallite size was determined from the X-ray line broadening using Scherrer relation with correction factor [126].

### **3.3.12 Microstructure**

Thin slices of slag corrosion tested samples were polished using various grades of abrasive papers and diamond paste. The microstructures of these samples were done using optical microscopy (LEICA, optical microscopy with image analyzer) at a magnification of 250.

The morphology of spinel nano powder was performed using scanning electron microscopy (SEM, model JSM 6480 LV JEOL, Japan). For the preparation of SEM sample, the powders were dispersed in isopropyl alcohol using ultra sonication bath (20 kHz, 500 W) for half an hour. One drop of the well-dispersed sample solutions were deposited on the glass slide. This glass slide was coated with platinum using sputtering and used for microscopy.

## Chapter 4

### *RESULTS AND DISCUSSION*

This chapter covers three sections. The first section describes the physical and chemical properties of micron-sized  $\text{MgAl}_2\text{O}_4$  spinel added MgO-C bricks. Three different types of micron-sized spinel such as AR-78, AR-90 and MR-66 were used in MgO-C bricks in order to standardize the type and amount of preformed spinel. The second section describes the characterization of nano  $\text{MgAl}_2\text{O}_4$  spinel, synthesized by citrate-nitrate method. The calcined  $\text{MgAl}_2\text{O}_4$  nanopowders were incorporated during fabrication of MgO-C bricks. The physical and chemical properties of nano-sized spinel added MgO-C bricks, without spinel as well as standardized spinel added MgO-C bricks are correlated in the third section.

## 4.1 Physical and chemical properties of micron-sized $\text{MgAl}_2\text{O}_4$ spinel added MgO-C bricks

### 4.1.1 AP, BD and CCS (before and after coking)

AP, BD and CCS of MgO-C refractories before and after coking with the addition of spinel types and amounts are given in Table 4.1, Table 4.2 and Table 4.3, respectively.

Table 4.1: AP (before and after coking) of MgO-C refractories with the addition of micron-sized spinel

Spinel type / amount	AP in % (before coking)				AP in % (after coking)			
	ZS	AR-78	AR-90	MR-66	ZS	AR-78	AR-90	MR-66
0	2.83	-	-	-	9.49	-	-	-
5	-	3.43	6.32	4.66	-	10.65	12.44	10.91
10	-	4.96	4.78	6.04	-	10.12	10.99	10.32
15	-	4.67	8.08	9.87	-	10.94	12.57	11.09
20	-	10.24	8.98	11.11	-	12.06	12.44	11.63
25	-	8.46	8.09	7.7	-	11.79	9.33	11.63

Table 4.2: BD (before and after coking) of MgO-C refractories with the addition of micron-sized spinel

Spinel type / amount	BD in g/cc (before coking)				BD in g/cc (after coking)			
	ZS	AR-78	AR-90	MR-66	ZS	AR-78	AR-90	MR-66
0	2.95	-	-	-	2.86	-	-	-
5	-	2.98	2.93	2.98	-	2.9	2.85	2.91
10	-	2.94	2.95	2.95	-	2.87	2.89	2.89
15	-	2.99	2.93	2.89	-	2.9	2.84	2.92
20	-	2.86	2.89	2.83	-	2.85	2.83	2.84
25	-	2.94	2.93	2.92	-	2.87	2.89	2.86

Table 4.3: CCS (before and after coking) of MgO-C refractories with the addition of micron-sized spinel

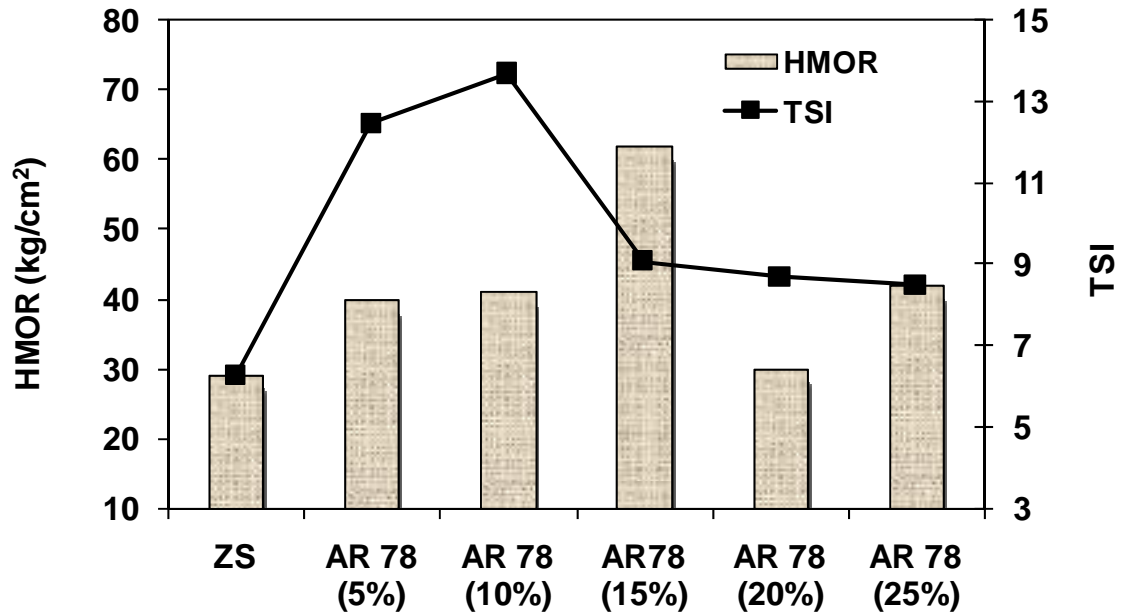
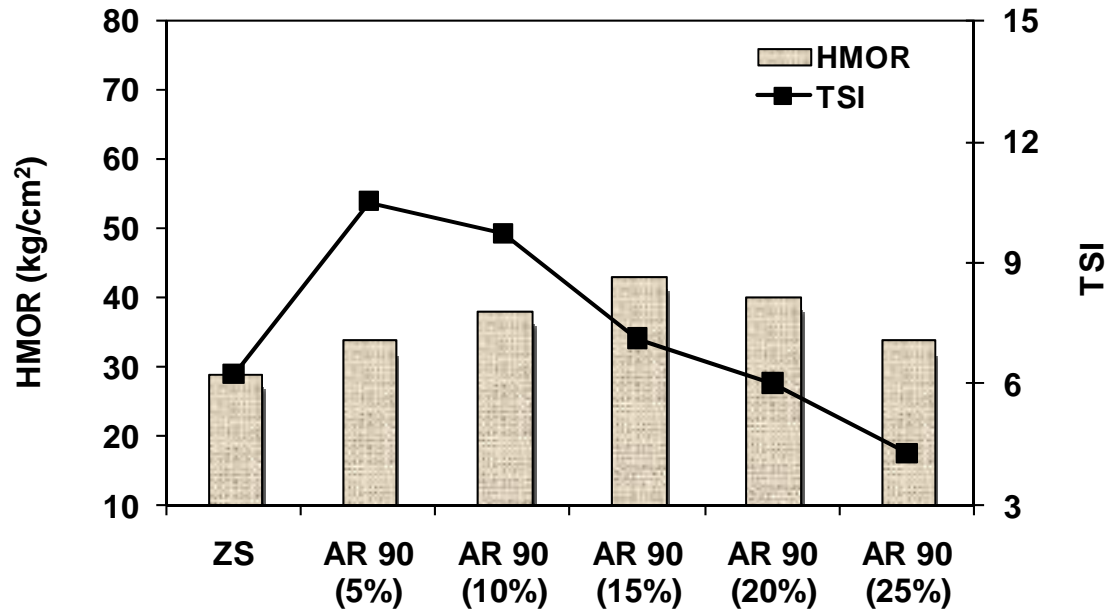
Spinel type / amount	CCS in $\text{kg/cm}^2$ (before coking)				CCS in $\text{kg/cm}^2$ (after coking)			
	ZS	AR-78	AR-90	MR-66	ZS	AR-78	AR-90	MR-66
0	284	-	-	-	220	-	-	-
5	-	310	278	289	-	169	145	134
10	-	418	378	326	-	174	207	165
15	-	363	309	363	-	217	108	202
20	-	249	285	254	-	103	150	128
25	-	262	267	314	-	148	138	153

With addition of spinel, the percentage of AP after coking was nearly two to three times more than that of AP before coking. The percentage of AP after coking was found to be nearly in the range of 10 % to 12 % (see Table 4.1). BD of MgO-C bricks before and after coking was in the range between 2.8 g/cc and 2.95 g/cc. However, the BD after coking was slightly lower as compared to BD before coking (see Table 4.2). As seen from the Table 4.3, the CCS value after coking was also lower as compared to CCS value before coking for different spinel added MgO-C bricks. The higher AP and lower BD as well as CCS after coking was due to the breaking of interlocking texture that has been created after polymerization of phenolic resin [127]. The breaking of the interlocking texture was due to the burning out of total organic portion of resin and release of harmful decomposition gases such as benzene, toluene, phenols and xylenol. [128, 129]. Thus the matrix phase was loosened thereby reducing strength of the bricks [47]. From AP, BD and CCS, it was still difficult to choose the appropriate spinel type and amount, so as to get better properties of MgO-C bricks. Thus, other physical and chemical characterizations of micron-sized spinel added MgO-C bricks have been done and the results are discussed in detail.

#### **4.1.2 HMOR and TSI**

Figure 4.1 shows HMOR and TSI as a function of different types and amounts of micron-sized spinel added MgO-C bricks. Higher HMOR was observed for micron-sized spinel containing bricks, when compared with ZS bricks. Irrespective of spinel addition, TSI of either 5 wt% or 10 wt% spinel added MgO-C brick was higher as compared to ZS bricks. The lowest HMOR value for AR-90 (5 wt%) was mainly due to the uncontrolled volume expansion caused due to in-situ spinel formation [93]. AR-78 (10 wt %) spinel added MgO-C bricks shows highest spalling index than the other spinel added bricks due to presence of micro-cracks (formed due to mismatch of thermal expansion co-efficient between magnesia and spinel) that acts as crack arresters, thus improving the TSI. However, the HMOR value of different types spinel (10 wt %) added MgO-C bricks was found to be around 40 kg/cm<sup>2</sup>. Highest HMOR was obtained for 15 wt % AR-78 spinel added MgO-C bricks. The reason for high HMOR was due to the formation of controlled in-situ spinel, thereby reducing pore size and resulting densification [93].

In addition to that, dispersion and retention of carbon after firing in the matrix of MgO-C refractory was effective in lowering their modulus of elasticity and thus improve the spalling resistance [130].



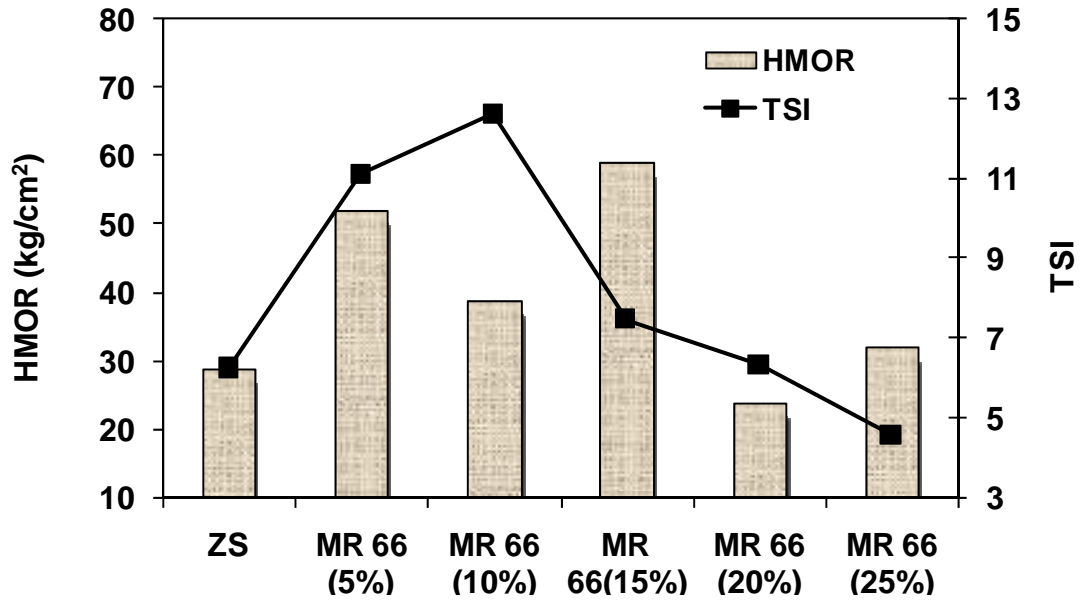


Fig. 4.1: HMOR and TSI as a function of different types and amounts of micron-sized spinel added MgO-C bricks

#### 4.1.3 Oxidation resistance

Figure 4.2 shows black surface remaining in percentage after oxidation resistance test for different spinel added MgO-C bricks. It was observed that the brick containing AR-78 spinel (10 wt % and 15 wt %) was the most effective in prevention of oxidation as compared to other spinel added MgO-C bricks. The results of oxidation tests in air are influenced by the permeability of decarburized layer. It was also possible that lower spinel content samples exhibited greater densification and higher strength after oxidation. Addition of spinel modifies the pore size distribution (reduces the number of large and channel pores) thereby hinders the entrance of oxygen into the matrix which ultimately results in high carbon retention. A similar type of phenomenon was also observed by Zhang et al [67] and Sen et al. [130].

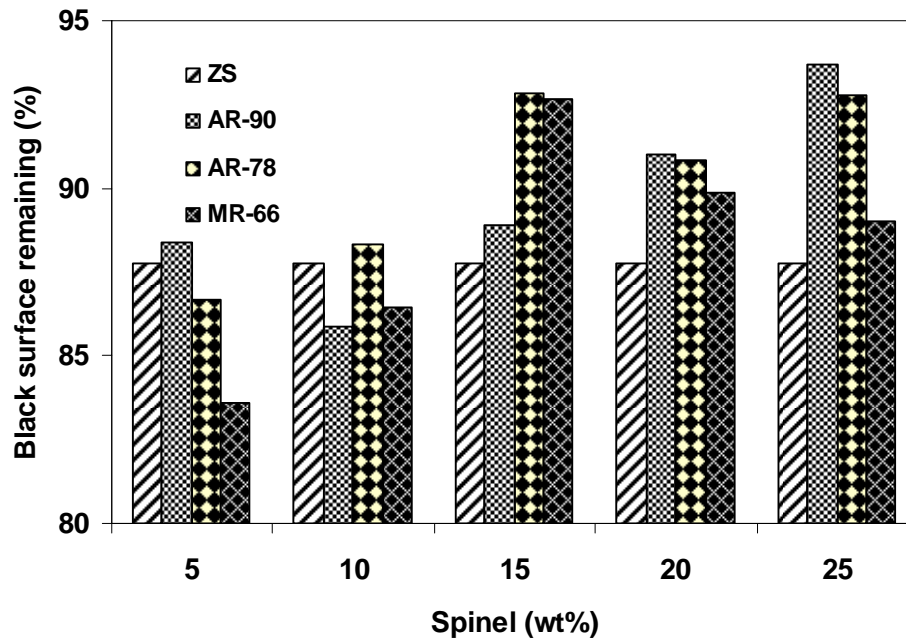


Fig. 4.2: Black surface remaining in % after oxidation resistance test for different bricks

#### 4.1.4. Rotary slag corrosion

Figure 4.3 shows the surface pattern of different spinel added MgO-C bricks after slag corrosion test. The rotary slag test result was clearly indicated that the incorporation of AR-78 spinel dramatically inhibits the slag corrosion and penetration resistance followed by MR-66 and AR-90 spinel addition. The inhibition of slag penetration by graphite can be simply observed from the residual slag coating on the surfaces of the slag tested bricks. In this present work, AR-78 spinel added in the form of fine powder ( $\sim 45 \mu\text{m}$ ) helps in retarding the slag intrusion and in consequence enhances the corrosion resistance of the MgO-C refractories. Fine spinel powders generally lead to better slag penetration resistance than the use of coarse grains as the distribution of fine spinel powder in the matrix was better and due to their high surface reactivity they can absorb ions such as  $\text{Fe}^{2+}$  and  $\text{Mn}^{2+}$  from slag and forming complex spinel more efficiently than coarse spinel grain [131]. The level of spinel addition also plays an important role in inhibiting slag penetration and corrosion resistance. If appropriate amounts of spinel are used, both slag penetration resistance and corrosion resistance of the refractory can be improved [82, 89, 132].

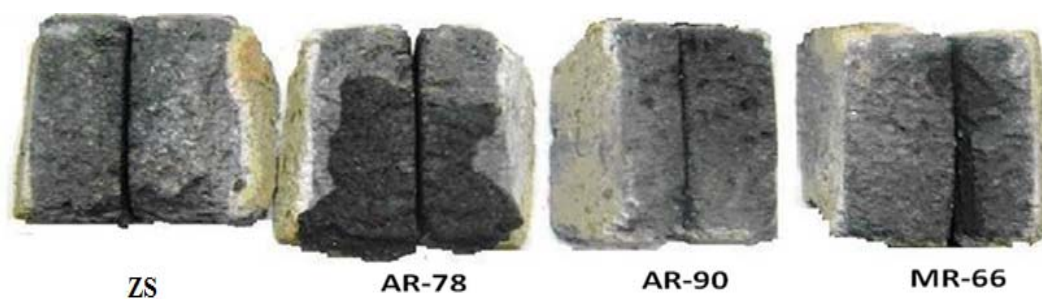


Fig. 4.3: Surface pattern of different spinel type MgO-C bricks after slag corrosion test

#### 4.1.5 Corrosion

Figure 4.4 shows corrosion (mm) as a function of different spinel added MgO-C refractories. It was clearly indicated that the AR-78 spinel added bricks had undergone lowest corrosion as it effectively depletes the slag of  $\text{Fe}^{2+}$  and  $\text{Mn}^{2+}$  cations, thereby making the slag more viscous, less penetration at the slag brick interface. It was seen from literature [82, 89, 132] that in-situ spinel formation in the matrix during application show excellent corrosion resistance in refractories. It was also seen that both slag penetration resistance and corrosion resistance of the refractory depend on the amounts of spinel.

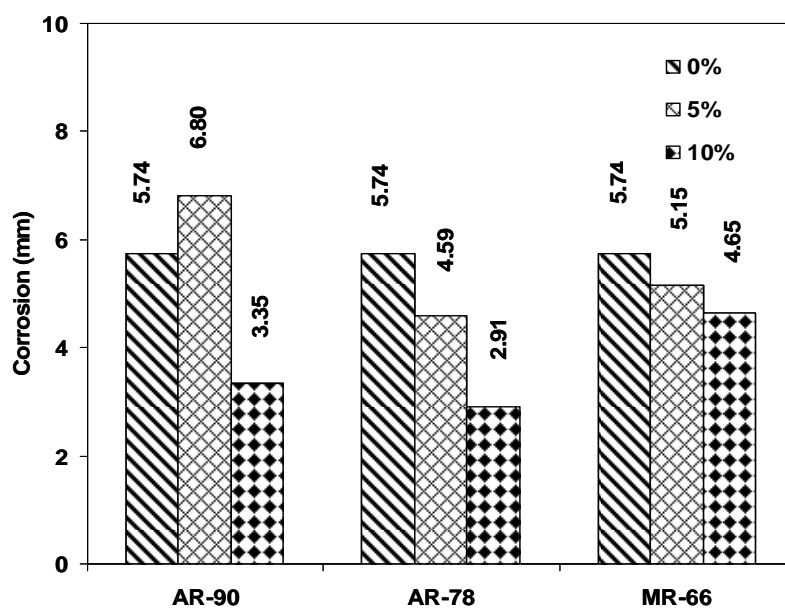


Fig. 4.4: Corrosion (mm) as a function of different spinel added MgO-C refractories



#### 4.1.6 Pore size distribution

The pore size distribution with average pore diameter of AR-78 and without spinel added MgO-C brick, after tempering is given in Table 4.4. It was observed that the average pore diameter of AR-78 was less as compared to without spinel added brick. Micron sized spinel present in the matrix occupies the pores and voids thereby decreasing the average pore diameter and improving the texture of the brick. The large pore ( $>70\text{ }\mu\text{m}$ ) distribution was more in without spinel added brick than AR-78 added brick. The larger pores of  $10\text{ }\mu\text{m}$  and above are the path for slag penetration which leads to penetration of slag into the bricks causing disintegration of MgO grains and finally dissolution of grains into the slag resulting in removal of the brick layer, which in turn determines the life of the ladle [133, 134]. The larger amount of fine pores ( $<1\text{ }\mu\text{m}$ ) provides an important boost in the brick strength as well as effectively restricts the slag penetration into pores. The emerging microstructure effectively reduces the slag corrosion of the product in service, as it was difficult for slag to penetrate into pores. At high temperatures, an organized microstructure with fine pores serves as an efficient heat insulator, which lowers heat losses of the ladle shell.

Table 4.4: Distribution of pores in MgO-C bricks after slag corrosion

Distribution of Pores (%)	MgO-C Bricks	
	ZS	AR-78 (10 wt %)
$< 0.1\text{ }\mu\text{m}$	5.38	4.73
$0.1\text{ }\mu\text{m}$	20.43	25.82
$1\text{ }\mu\text{m}$	67.38	64.00
$10\text{ }\mu\text{m}$	4.30	3.27
$> 70\text{ }\mu\text{m}$	2.51	2.18
Average pore diameter ( $\mu\text{m}$ )	0.3149	0.1309

#### 4.1.7 Microstructure

A typical normal and large crystal of 97 % fused magnesia grains are shown in Fig. 4.5 (a) and (b), respectively. The grain size of large crystal was in the range of 500  $\mu\text{m}$  to 1000  $\mu\text{m}$ . The larger size of the periclase crystals have lower the wear rate and better the corrosion resistance [58, 59].

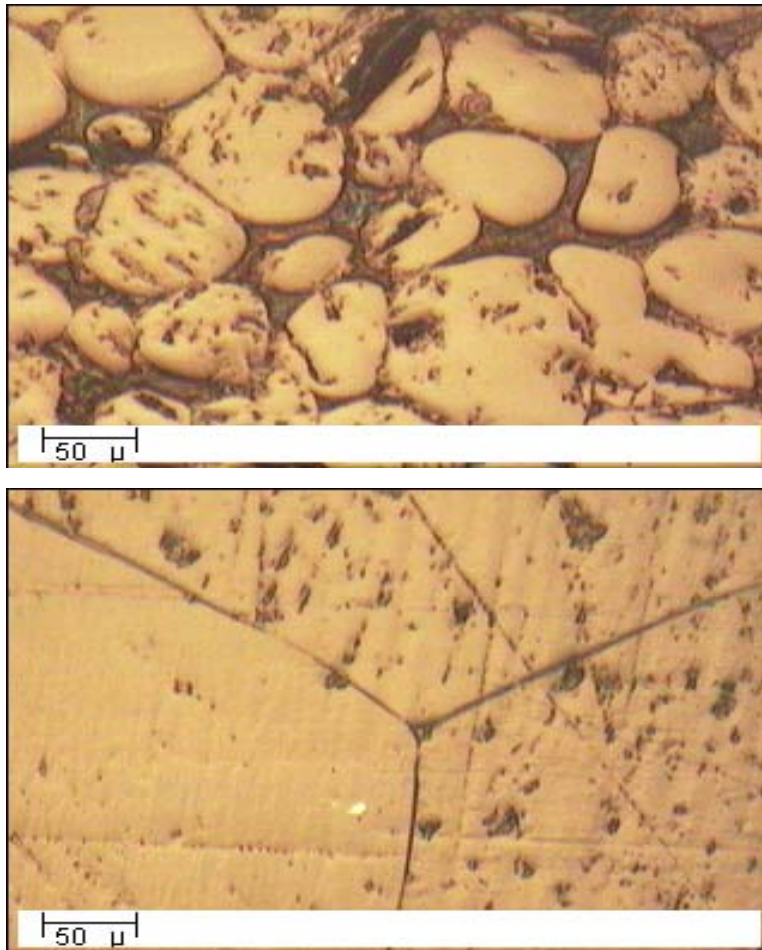


Fig. 4.5: Optical micrographs of (a) normal and (b) large crystal of 97 % fused MgO

Figure 4.6 show optical micrographs of without spinel added MgO-C bricks which indicate (a) crack formation and (b) disintegration of MgO grains after rotary slag corrosion test. When the slag comes and contact with MgO-C brick, fracture and disintegration of MgO grains took place due to thermo mechanical stress [100].

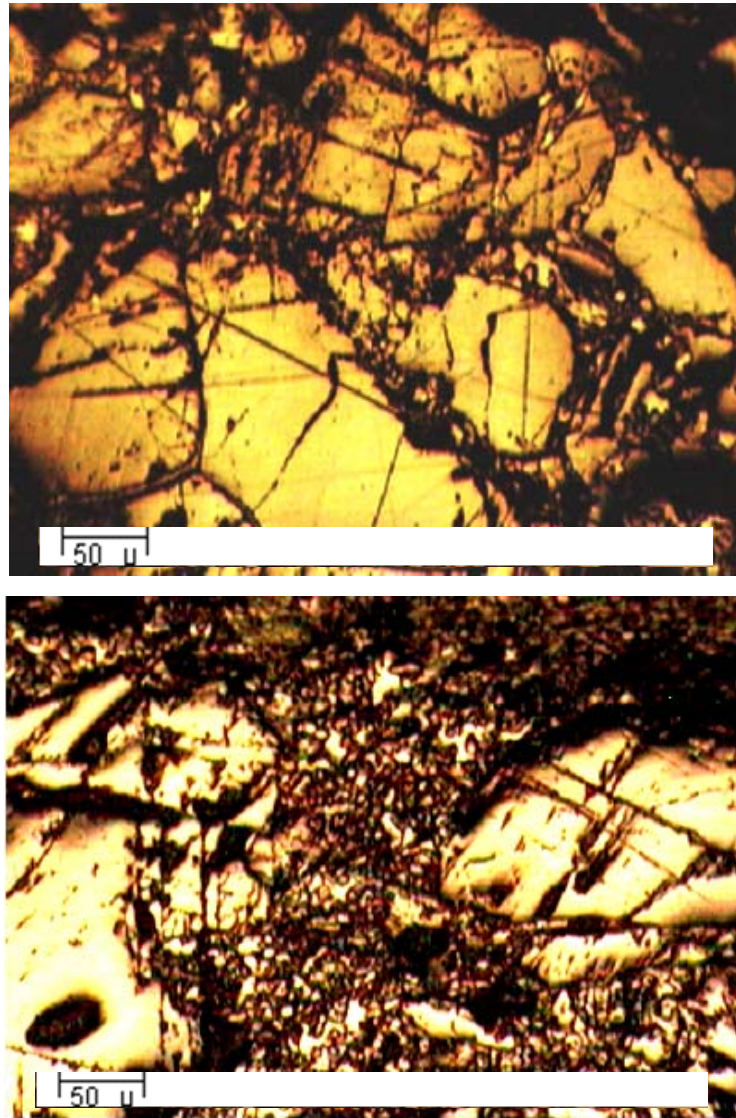


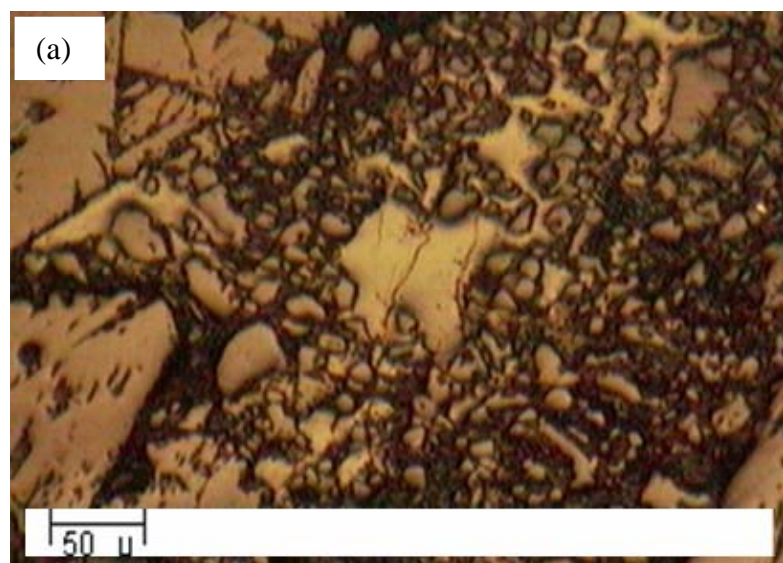
Fig. 4.6: Optical micrographs of MgO-C bricks without spinel addition after slag corrosion test which indicate (a) Crack formation and (b) disintegration of MgO grains.

The presence of graphite in the matrix after slag corrosion test for AR-78 (10 wt%) spinel added an MgO-C brick was clearly observed from the optical micrograph of the slag-refractory interface which was shown in Fig. 4.7. The slag has penetrated the refractory material in pores and cracks. The corrosion of oxides often occurs not only by dissolution or evaporation of oxide, but also by the penetration of slag into the pores of the brick. The slag penetrates into the open pores by capillary forces and the solid from the slag diffuses both through the grain boundaries and into the bulk of the solid [100].



Fig.4.7: Optical micrograph shows graphite intact for AR-78 spinel added MgO-C bricks after slag corrosion test

Figure 4.8 (a) and (b) shows the optical micrographs of without spinel and AR-78 spinel added MgO-C bricks after rotary slag corrosion test, respectively.





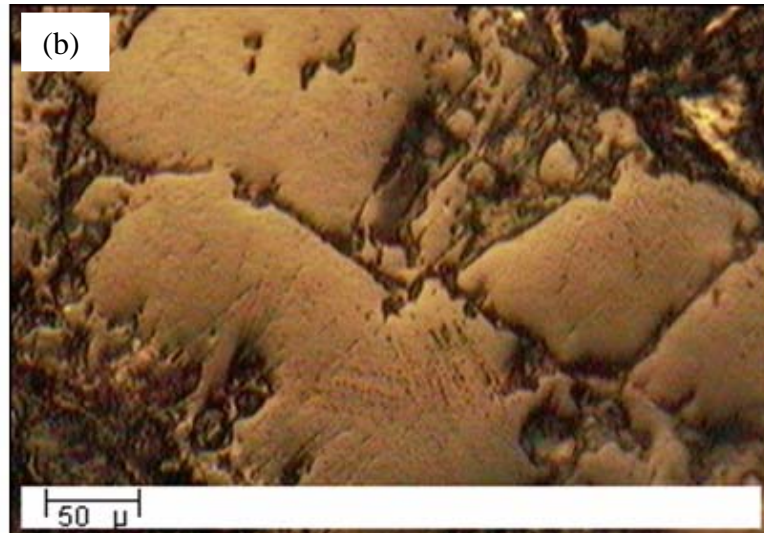


Fig. 4.8: Optical micrographs of MgO-C bricks (a) without spinel and (b) with AR-78 spinel after slag corrosion test

Dissolution of MgO grains into slag was high in case of without spinel added MgO-C brick (see Fig. 4.8 a). However, retention of graphite in the matrix and less dissolution of MgO grains were observed in AR-78 added MgO-C brick (see Fig. 4.8 b). Slag coating was also observed in case of AR-78 added MgO-C brick thereby hindering further penetration.

#### 4.1.8 Summary

- Out of the three different spinels (AR-90, AR-78 and MR-66) added MgO-C bricks, AR-78 (10 wt %) spinel added MgO-C brick exhibits better thermal spalling resistance, corrosion and oxidation resistance as compared to that of AR-90 or MR-66 spinel added MgO-C bricks.

## 4.2 Characterization of $\text{MgAl}_2\text{O}_4$ spinel nanopowders synthesized by citrate-nitrate method

### 4.2.1. Thermal analysis

Figure 4.9 shows DSC-TG curve of the gel. The weight of the gel decreases as the temperature increases. The initial  $\sim 12\%$  weight loss, which occurs from room temperature to  $150^\circ\text{C}$  was due to the removal of free water molecules and volatile residues present in the precursor sample. This weight loss was supported by the presence of endothermic peak in DSC curves at  $\sim 122^\circ\text{C}$ . The second and major weight loss of around  $30\%$  in the temperature range  $150^\circ\text{C}$  to  $900^\circ\text{C}$  was associated with a broad exothermic effect. The spinel phase formation was observed by an exothermic peak in the temperature range from  $700^\circ\text{C}$  to  $850^\circ\text{C}$  as seen in DSC curves. For further confirmation of the phase transformation behavior, the as-prepared amorphous spinel powders were heat-treated at different temperatures and phase analysis was done by XRD.

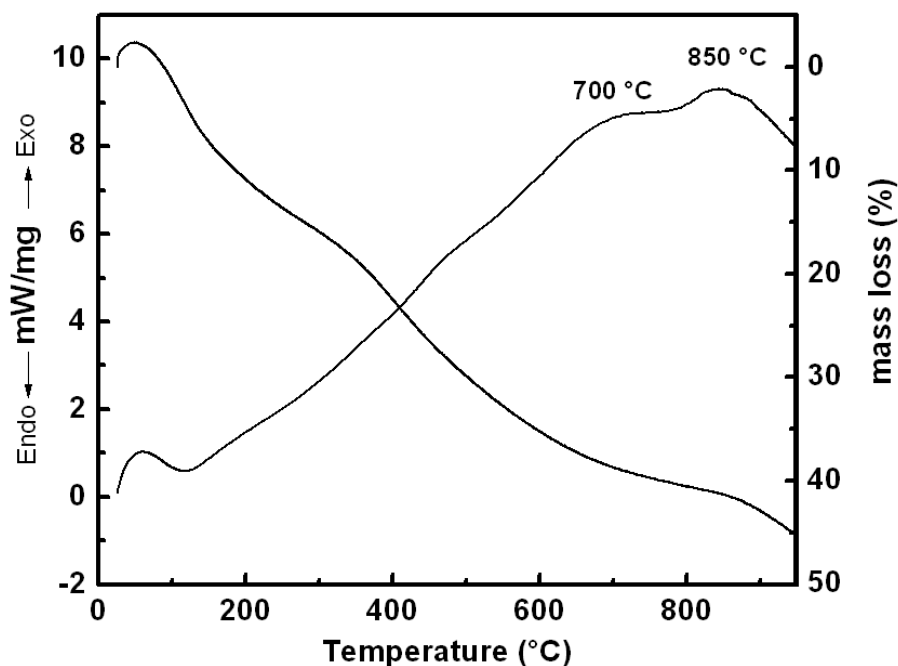


Fig. 4.9: DSC-TG curve of the gel

#### 4.2.2. Structure and microstructure

Figure 4.10 shows the XRD patterns of the as-prepared spinel powder heat-treated at 600 °C, 700 °C and 800 °C for 5h. It was observed that the spinel powder was in amorphous nature up to 600 °C. The spinel phase formation starts at 700 °C and pure  $\text{MgAl}_2\text{O}_4$  powder with crystallite size of around 15 nm was found to be formed at 800 °C.

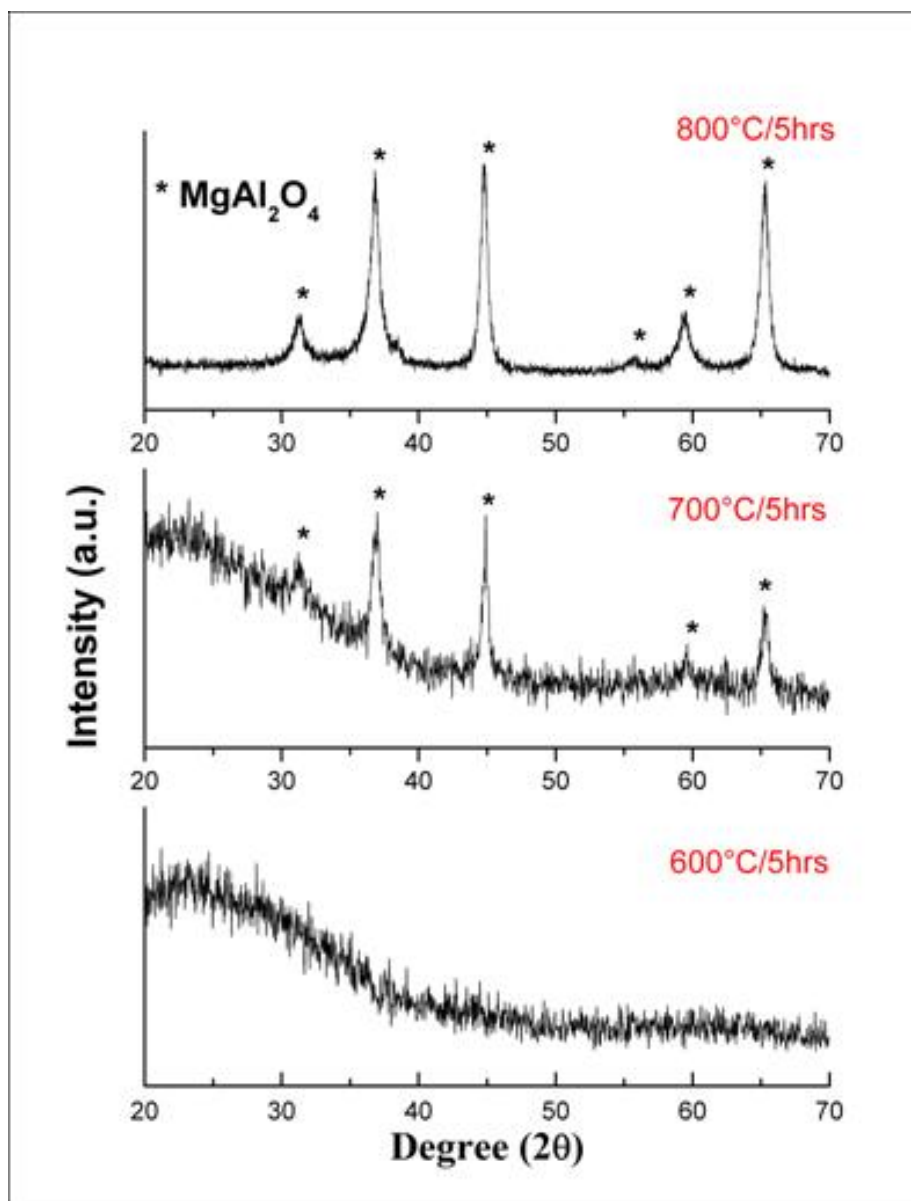


Fig.4.10: XRD patterns of as-prepared spinel nanopowders calcined at different temperatures

In order to get a direct and complete picture of the morphology, SEM was performed for  $\text{MgAl}_2\text{O}_4$  nanopowders. Figure 4.11 shows SEM micrograph of calcined (800 °C)  $\text{MgAl}_2\text{O}_4$  nanopowder. The particles size was found to be in the range of 50 nm to 100 nm.

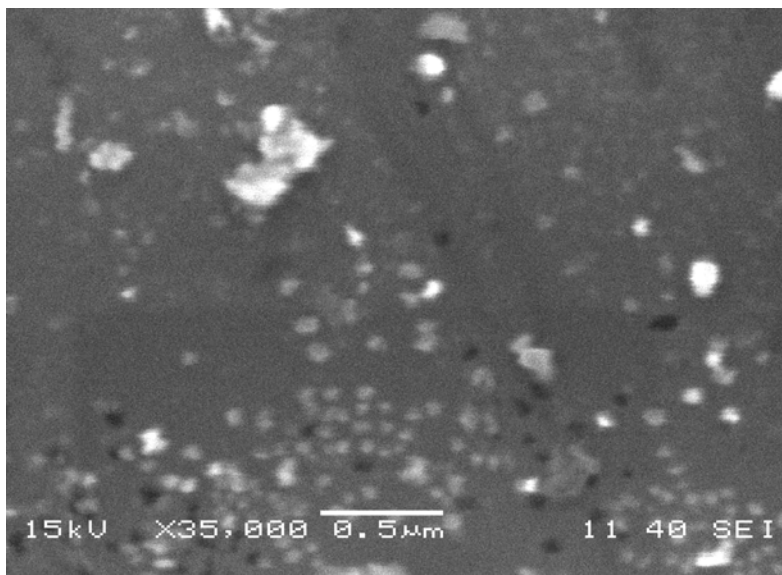


Fig.4.11: SEM micrograph of  $\text{MgAl}_2\text{O}_4$  nanopowder

#### 4.2.3 Surface area

The surface area of the synthesized spinel powder calcined at 800°C for 5 hrs was found to be nearly  $56 \text{ m}^2\text{g}^{-1}$ , which is equivalent to a crystallite size of 15 nm. The measured surface area was converted to equivalent particle size of 33 nm.

#### 4.2.4 Summary

Nanocrystalline  $\text{MgAl}_2\text{O}_4$  spinel powder was successfully synthesized through citrate-nitrate process. The initial crystallization temperature of the  $\text{MgAl}_2\text{O}_4$  spinel powder was 700°C. Pure  $\text{MgAl}_2\text{O}_4$  spinel formation took place at around 800 °C. The measure surface area was found to be around  $56 \text{ m}^2\text{g}^{-1}$ . The crystallite size of  $\text{MgAl}_2\text{O}_4$  was found to be around 15 nm. The calcined nanopowders with different concentration were incorporated in MgO-C refractory and the properties of these refractory are discussed in next section.



### 4.3 Physical and chemical properties of without, standardized and nano-sized $\text{MgAl}_2\text{O}_4$ spinel added MgO-C refractory

#### 4.3.1 AP, BD and CCS (before and after coking)

AP, BD and CCS of nano-sized  $\text{MgAl}_2\text{O}_4$  added MgO-C refractories before and after coking are given in Table 4.5. These results were correlated with the results of ZS and standardized micron-sized 10 % AR-78 spinel added MgO-C refractories.

Table 4.5: AP, BD and CCS of nano-sized  $\text{MgAl}_2\text{O}_4$  spinel added MgO-C refractories, correlated with ZS and AR-78 added MgO-C refractory.

Spinel amount/ type	Before coking			After coking		
	AP in %	BD in g/cc	CCS in $\text{Kg/cm}^2$	AP in %	BD in g/cc	CCS in $\text{kg/cm}^2$
ZS	4.03	2.94	398	9.13	2.89	227
10% AR78	3.25	2.92	455	8.23	2.87	266
0.1% NS	4.18	2.95	394	10.25	2.90	235
0.5% NS	2.97	2.96	482	8.01	2.90	278
1.0% NS	2.88	2.95	495	7.87	2.90	288
1.5% NS	4.28	2.94	403	11.89	2.89	240

The percentage of AP for ZS and AR-78 added spinel MgO-C bricks was found to be around 8 % to 9 % after coking which was nearly two to three times more than AP before coking. With addition of nano spinel in MgO-C refractory, the percentage of AP varies from 7 to 11 after coking. The higher value of AP may be due to changes in granulometry and lower value of AP may be due to densification. However, the BD value was not varied with nano spinel addition and found to be in the range between 2.87 to 2.95 g/cc. CCS after coking was better for the refractory containing 0.5 % and 1 % nano spinel added refractory. The use of nanoparticles reduces the AP and increases the CCS of the refractory as compared to ZS and micron-sized AR-78 spinel added bricks. This may be due to the reason that nano-particles and resin binder disperses among the spaces between the coarse, medium and fine particles of the refractory matrix. Additives as well as other miscellaneous materials consequently play a role by filling up the interior pores and gaps between various particles. [21]. However with increase in nano spinel amount

beyond 1 wt% in the matrix part builds up a “bridge” structure results in reduction in strength and increase in apparent porosity. The similar kind of phenomena was observed while adding above 1wt% of nano calcium carbonate in corundum based castables [135]. Hence, it was more interesting to characterize the other physical and chemical properties of these nano spinel added MgO-C refractory.

#### 4.3.2 HMOR and TSI

Figure 4.12 shows HMOR and TSI as a function of nano spinel added MgO-C refractory. Highest HMOR and TSI were obtained for AR-78 (10 wt %) spinel and 1 wt % nano spinel added MgO-C refractory. This may be due to the dispersion of nano-sized spinel in the matrix that protects the carbon [130, 18, 136]. Higher amount of carbon retention was observed by the addition of spinel in the brick which lead to lowering of MOE values. Retention of carbon after firing in the matrix of MgO-C refractory was effective in lowering their modulus of elasticity and was therefore expected to improve their spalling resistance.

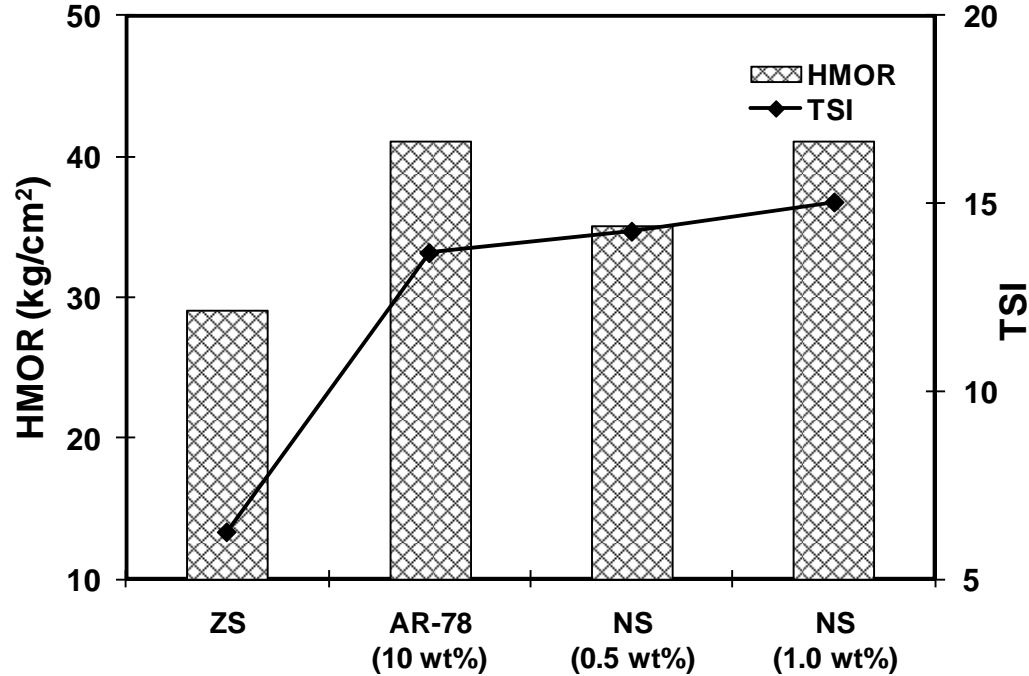


Fig. 4.12: HMOR and TSI as a function of spinel added MgO-C refractory

### 4.3.3 Oxidation resistance

Figure 4.13 shows black surface remaining (%) after oxidation resistance test for nano spinel added MgO-C refractory. It was observed that the brick containing nano spinel was most effective in prevention of oxidation as compared to without spinel added or AR-78 spinel added samples due to its high reactivity and high surface area [82; 131]. Better oxidation resistance was obtained for the MgO-C refractory containing 0.5 wt % and 1 wt % nano spinel.

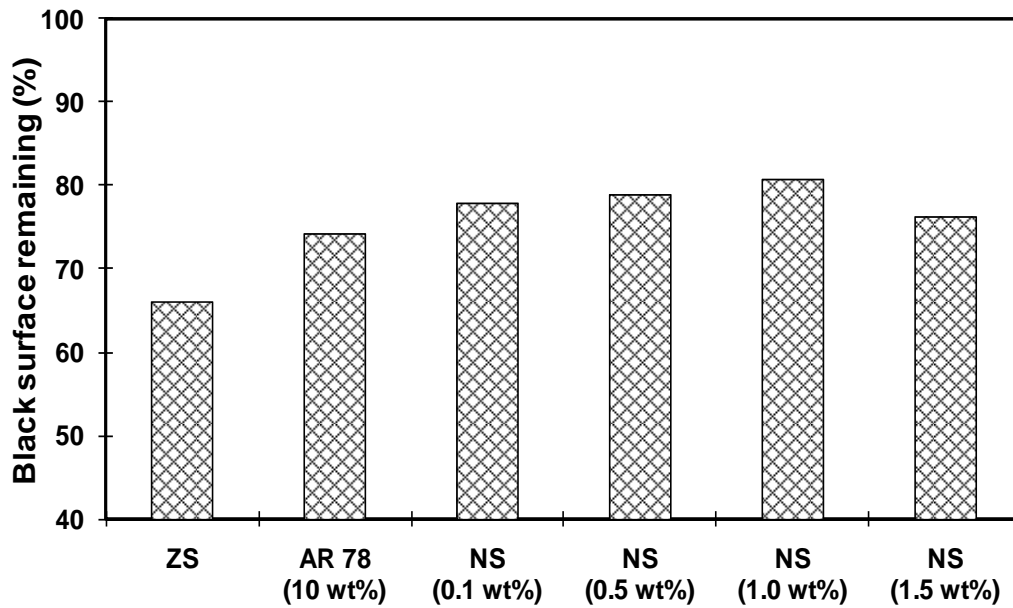


Fig. 4.13: Black surface remaining in % as a function of spinel addition in MgO-C refractory

### 4.3.4. Static crucible slag corrosion

Fig.4.14 shows the cross section of the refractory containing without and with spinel (micron as well as nano) after slag corrosion test. Incorporation of nano spinel (0.5 and 1 %) dramatically inhibits the slag corrosion and penetration resistance followed by without and AR-78 spinel addition. Spinel being a defective structure, always has a tendency of substitutional solid solution by accommodating the  $\text{Fe}^{2+}$  and  $\text{Mn}^{2+}$  and  $\text{Ca}^{2+}$  ions from the slag in its defect structure making the slag more viscous and less

penetrative. Hence the penetration of slag is reduces which inturn improve the corrosion resistance. This effect is more predominant when the particle size of spinel decreases to nano level as the reactivity, surface area and surface volume increase by many folds. Nano spinel being very fine in nature possesses high reactivity, high surface area and specific volume thereby forming a coating on the surface of graphite leading to prevention of decarburisation of graphite from the matrix [82, 131]. Hence, addition of 0.5 wt % and 1 wt% nano spinel in MgO-C refractory exhibits higher oxidation thereby leading to better slag corrosion and penetration resistance.

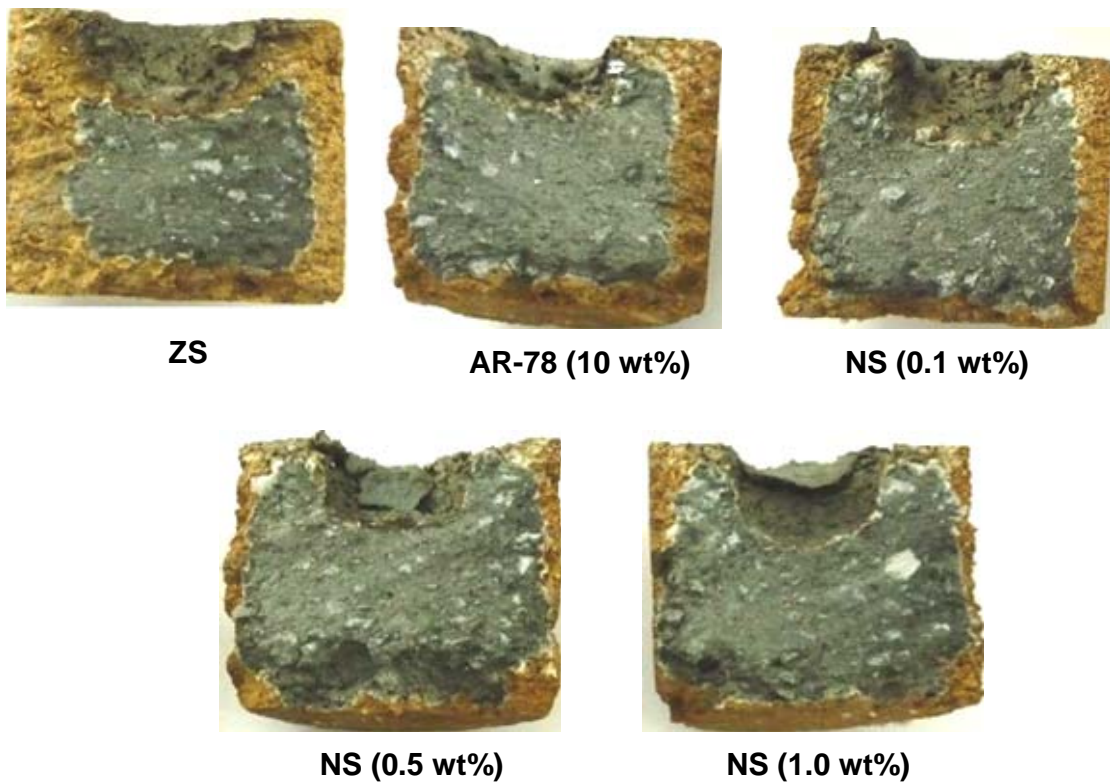


Fig. 4.14: Surface pattern of different spinel type MgO-C samples after slag corrosion test

#### 4.3.5 Corrosion

Figure 4.15 shows corrosion (mm) as a function of spinel added MgO-C refractories. It was clearly indicated that the 1 wt % nano spinel added refractory had undergone lowest corrosion than the other type of spinel added bricks. Fine spinel

powders generally lead to better slag penetration resistance than the use of coarse grain due to its high surface reactivity [82]. Nano spinel powders can take up slag ions such as  $\text{Fe}^{2+}$  or  $\text{Mn}^{2+}$  and dissolve more efficiently than the coarse spinel grain [131]. Zhang et al., [67] reported that the spinel in the matrix of MgO-C refractory could effectively protect the graphite against oxidation by bonding the graphite flakes, and subsequently increase the corrosion resistance. This also maintained the integrity of the refractory texture and thus inhibits further slag penetration and subsequent corrosion. Hence refractories with spinel addition demonstrate a better corrosion resistance along with matrix densification as compared to bricks without spinel addition. Addition of nano spinel further leads to densification of texture owing to its finer size and surface reactivity. Several papers have reported that the type, size and amount of spinel addition play an important role in inhibiting slag penetration and corrosion resistance [82, 89, 132].

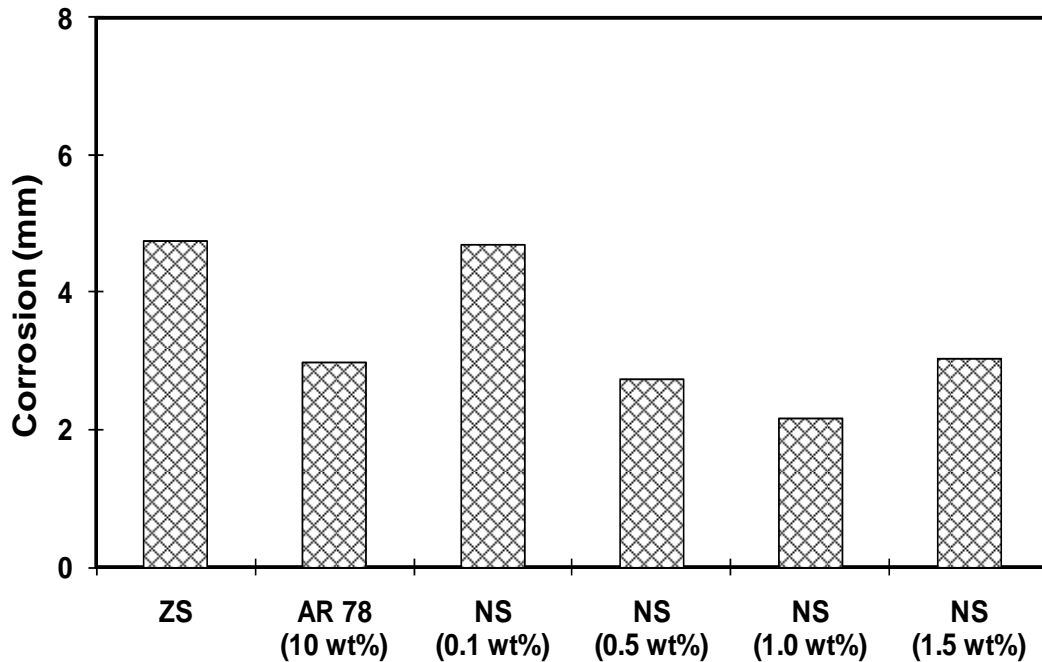


Fig. 4.15: Corrosion (mm) as a function of spinel added MgO-C refractories

#### 4.3.6 Pore size distribution

Table 4.6 shows the distribution of pores and average pore diameter of without spinel, AR-78 and nano spinel added refractory after tempering. Pore size and number of pore was decreased by maintaining a uniform size distribution by incorporating a small amount of nano-sized spinel in the matrix of refractory. The nano-sized spinel goes into the pores and in between the macron-sized magnesia and graphite particles. As a result, the pore size and number of pores are reduced and hence a uniform pore size distribution was created in the matrix [130]. The average pore diameter for 1 wt % nano spinel added MgO-C brick was found to be less as compared to without and 10 wt % AR-78 added spinel bricks.

Table 4.6: Distribution of pores in spinel added MgO-C refractories after slag corrosion

Properties		0% ZS	10% AR-78	0.5% NS	1% NS
Avg. pore dia. ( $\mu\text{m}$ )		0.2763	0.1309	0.1237	0.0804
Pore size distribution	< 0.1 $\mu\text{m}$ (%)	9.48	19.17	16.03	22.37
	0.1 – 1 $\mu\text{m}$ (%)	38.24	48.33	48.09	46.49
	1-75 $\mu\text{m}$ (%)	48.69	30	33.21	28.95
	>75 $\mu\text{m}$ (%)	3.27	2.08	2.29	1.75

#### 4.3.7 Microstructure

Figure 4.16 (a) and (b) shows the optical micrographs of 0.5 % and 1 % nano spinel added MgO-C refractory, respectively after rotary slag corrosion test. Dissolution of MgO grains into slag was observed in both without spinel and AR-78 spinel added MgO-C brick [see Fig. 4.8 (a) and (b)]. However, with addition of 1 wt % nano spinel restricted dissolution of MgO grains as well as retention of carbon in the matrix (see Fig. 4.16 b), thus gives better corrosion resistance.

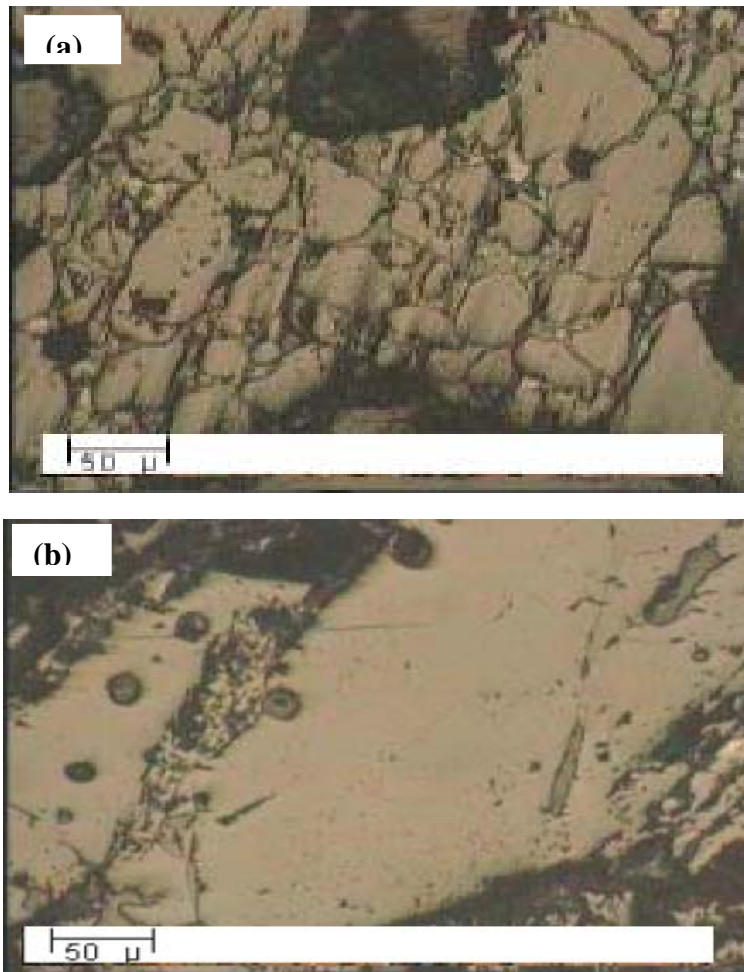


Fig. 4.16: Optical micrographs of (a) 0.5 % and (b) 1 % nano spinel added MgO-C refractories after slag corrosion test.

#### 4.3.8 Summary

- The average pore diameter was less for 1 wt % nano spinel added MgO-C refractory as compared to ZS and AR-78 added spinel bricks. Large pores (1-75  $\mu\text{m}$  and above) are less in case of 1 wt % nano spinel added brick as compared to others.
- Low corrosion rate was observed in case of 0.5 wt % and 1 wt% nano spinel added refractory.
- 0.5 wt % and 1 wt % nano spinel addition in MgO-C refractory gives better HMOR, TSI and corrosion as well as oxidation resistance as compared to that of ZS and AR-78 added bricks.

## **Chapter 5**

### *CONCLUSIONS*



The present work deals with the improvement of physical and chemical properties of MgO-C bricks with the addition of micron and nano-sized  $\text{MgAl}_2\text{O}_4$  spinel. The significant findings of this work are

- Oxidation, slag penetration and thermal spalling resistance of near stoichiometric spinel (10 wt% AR-78) added MgO-C refractory brick properties are found to be superior than AR-90, MR-66 and without spinel added bricks, which generally determine the life of the ladle. This was due to the presence of large amount of fine pores and modification of pore size distribution by spinel addition and effectively depleting the divalent cations ( $\text{Fe}^{2+}$ ,  $\text{Mn}^{2+}$ ) from the slag coming in contact with the brick surface thereby making the slag more viscous and less penetrative which in turn helped in prevention of slag penetration.
- Carbon retention in AR-78 (10 wt %) spinel added brick was high (observed from oxidation test) as compared to AR-90, MR-66 and without spinel added MgO-C bricks. Thus, spinel addition helped in preventing decarburization of graphite present in the brick.
- Slag coating on AR-78 added MgO-C bricks (observed from rotary slag corrosion test) led to further prevention of penetration of slag into brick.
- AR-78 (10 wt%) spinel added bricks possesses greater degree of thermal spalling resistance as compared to other spinel or without spinel added bricks. This was due to mismatched thermal expansion coefficient between spinel and magnesia which led to the formation of voids and micro cracks in the refractory body. The voids and micro cracks present in the matrix acts as crack arresters, thereby improving the thermal spalling resistance of bricks.
- The nano-sized  $\text{MgAl}_2\text{O}_4$  spinel was synthesized using citrate-nitrate route and the crystallite size and particle size was found to be around 15 nm (calculated from XRD) and 32-50 nm (observed from SEM) respectively at 800 °C. These powders were used in fabrication of nano spinel added MgO-C bricks. The average pore diameter was less in nano spinel added MgO-C bricks as compared to micron spinel

bricks. The carbon retention was higher in nano spinel added MgO-C bricks. Thus nano spinel (0.5 wt % and 1 wt %) added bricks gives better HMOR, TSI, oxidation and slag corrosion resistance as compared to AR-78 or without spinel added bricks.

- Graphite retention and corrosion resistance has been improved by many folds with the addition of nano spinel as compared to without spinel and 10 wt% AR-78 spinel added bricks which was clearly observed from optical micrographs.

Finally, this research work clearly shows the potential of micron and nano  $\text{MgAl}_2\text{O}_4$  spinel added MgO-C bricks for the application in the slag lines of ladle metallurgical furnace.

### **SCOPE FOR FUTURE WORK**

The results so far obtained are highly encouraging and the main suggestions for scope for future work are as follows:

- Exploration of different sources to get bulk amount of nano spinel.
- Field trials to be carried out with the developed AR-78 spinel added MgO-C bricks in steel ladle.
- Use of cost effective prespin (preformed spinel) in MgO-C refractories and study its effect on the physical and chemical properties.
- Mixing of nano spinel along with other ingredients of MgO-C brick in the mixture machine was very difficult and cumbersome. So innovative technology was to be developed to ease the incorporation of nano spinel in MgO-C refractory system.

## References

1. Zamboni, L.A., and Caligaris, R.E., "Different compositions of MgO-C bricks used in ladle slag line". Proc. UNITECR'97, New Orleans, USA, pp.765–773 (1997).
2. Aneziris, C.G., Borzov, D., and Ulbricht, J., "Magnesia carbon bricks-a high-duty refractory material", Inter. Ceram Refract. Man., pp.22–27 (2003).
3. Annual book of ASTM standards, Refractories: Activated carbon, Advanced ceramics, 15.01, pp.19 (2003).
4. Kingery, W.D., Bowen, H.K., and Uhlmann, D.R., "Introduction to Ceramics". John Wiley and Sons, New York, (1976).
5. Tassot, P., Etienne, F., Wang, J., and Atkinson, P., "New concepts for steel ladle linings", Proc. UNITECR'07, Dresden, Germany, pp.462-465 (2007).
6. Inuzuka, T., "Technical development of refractories for steel making process", Nippon steel technical report No: 98, pp.63-69 (2008).
7. Exenberger, R., Moser, H., Niederhammer, K., Heiss, J., and Hoefer, W., "Improvement of the refractory lining in the ld- converter at voestalpine Stahl GmbH LINZ, Australia", Proc. UNITECR'07, Dresden, Germany, pp.73-76 (2007).
8. Majumdar, S., "Improvement in lining life", Advances in refractories for steel making, 2007, RDCIS, Ranchi.
9. Barua, P., "Experiences in BOFs and steel ladles at SMS-II, RSP", Advances in refractories for steel making, RDCIS, Ranchi (2007).
10. Gruber, D., Auer, T., and Harmuth, H., "Influence of an irreversible expansion of a teeming ladle lining on its thermo-mechanical behaviour", 51<sup>st</sup> Intl. Colloq. on Refractories, Aachen, Germany, pp.73-75 (2008).
11. Figueiredo Jr, A., Bellandi, N., Vanola, A., and Zamboni, I., "Technological evolution of magnesia-carbon bricks for steel ladles in Argentina", Iron and Steel Technology, 1 pp.42-47 (2004).
12. Buchebner, G., Sampayo, L., Samm. V., Blondot, P., Peruzzi, S., and Boulanger, P., "ANKERSYN – A new generation of carbon-bonded magnesia carbon bricks", RHI Bulletin, pp.24-27 (2008).

13. Kuffa, T., Sucik, G., and Hrsak, D., "The influence of carbon materials on the properties of MgO refractories", *Materials and Technology*, 39, pp.211-213(2005).
14. Chatterjee, S., and Eswaran, R., "Continual improved performance MgO-C refractory for BOF", *Proc. UNITECR'09*, Salvador, Brazil, Article ID.136 (2009).
15. Ganesh, I., Bhattacharjee, S., Saha, B.P., Johnson, R., Rajeshwari, K., Sengupta, R., Ramana Rao, M.V., and Mahajan, Y.R., "An efficient  $\text{MgAl}_2\text{O}_4$  spinel additive for improved slag erosion and penetration resistance of high- $\text{Al}_2\text{O}_3$  and MgO-C refractories", *Ceram. Int.*, 28, pp.245 – 253 (2002).
16. Sarpoolaky, H., Zhang, S., and Lee, W.E., "Corrosion of high alumina and near stoichiometric spinels in iron-containing silicate slags", *J. Euro. Ceram. Soc.*, 23, pp.293-300 (2003).
17. Bavand-Vandchali, M., Sarpoolaky, H., Golestani-Fard, F., and Rezaie, H.R., "Atmosphere and carbon effects on microstructure and phase analysis of in-situ spinel formation in MgO-C refractories matrix", *Ceram. Int.*, 35, pp.861-868 (2008).
18. Bavand-Vandchali, M., Golestani-Fard, F., Sarpoolaky, H., Rezaie, H.R., and Aniziris, C.G., "The influence of in-situ spinel formation on microstructure and phase evolution of MgO-C refractories", *J. Euro. Ceram. Soc.*, 28, pp.563-569 (2008).
19. Tamura, S-I., Ochiai, T., Takanaga, S., Kanai, T-A., and Nakamura, H., "Nano-tech. refractories – 1: The development of the nano structural matrix", *Proc. UNITECR'03*, Osaka, Japan, pp.517-520 (2003).
20. Takanaga, S., Ochiai, T., Tamura, S., Kanai, T., and Nakamura, H., "Nano-tech. Refractories – 2: The application of the nano structural matrix to MgO-C bricks", *Proc. UNITECR'03*, Osaka, Japan, pp.521-524 (2003).
21. Ochiai, T., "Development of refractories by applying nano-technology", *TARJ*, 25, pp.4-11 (2005).
22. Harada, T., Matsuura, O., Uchida, M., and Takahashi, H., "Comparison of the characteristics of MgO-C brick formed by different pressing methods", *TARJ*, 21, pp.172-176 (2001).
23. Blumenfeld, P., Peruzzi, S., Puillet, S., and de Lorgeril, J., "Recent improvements in Arcelor steel ladles", *La Revue de Metallurgie- CIT*, 3, pp. 233-239 (2005).

24. Sickafus, KE., Wills, JM., Grimes, NW, "Structure of Spinel", J. Am. Ceram. Soc., 82, pp.3279 – 3292 (2004).
25. Ghosh, B., Chakrabarty, P., Pal, P.G., Mitra, S.K., Swaminathan, K.S., "Magnesio-aluminate spinel – a potential raw material for making new generation refractories", Proc. UNITECR'95, Kyoto, Japan, pp.541-549 (1995).
26. Korgul, P., Wilson, D.R., and Lee, W.E., "Microstructure analysis of corroded alumina-spinel castable refractories", J. Euro. Ceram. Soc., 17, pp.77-84 (1997).
27. Lee, W.E., Korgul, P., Goto, K., and Wilson, D.R., "Microstructural analysis of corrosion mechanisms in oxide-spinel steel making refractories, Proceedings of the 2<sup>nd</sup> International symposium on advances in refractories for the metallurgical industries, II, pp.453-465 (1996).
28. Zhang, S., Lee, W.E., Spinel containing refractories, Handbook of refractories, Marcel Dekker Inc., USA, pp.215-257 (2004).
29. Sumimura, H., Yamamura, T., Kubota, Y., and Kaneshige, T., "Study on slag penetration of alumina-spinel castable", Proc. UNITECR'97, New Orleans, USA, pp.97-101, (1997).
30. Matsumoto, O., Isobe, T., Nishitani, T., and Genba, T., "Alumina-spinel monolithic refractories". US Patent 4 990 475 (1991).
31. Kurata, K., Matsui, T., and Sakki, S., "Castable lining technique to bottom of teeming ladle", Taikabutsu Overseas, 12, pp.29-39 (1992).
32. Tao, S.P., Li, W.X., and Cao, Y., "Application of spinel carbon brick in steel ladle", Proc. UNITECR'95, Kyoto, Japan, pp.286-289 (1995).
33. Gleiter, H., "Nanocrystalline materials: basic concept and microstructure", Acta Mater., 48 (2000), pp.1-29;
34. Tjong, S., and Chen, H., "Nanocrystalline materials and coatings", Mater. Sic. Eng. Res., 45, pp.1-88 (2004).
35. Chen, M., Lu, C., and Yu, J., "Improvement in performance of MgO-CaO refractories by addition of nano-sized ZrO<sub>2</sub>", J. Euro. Ceram. Soc., 27, pp.4633-4638 (2007).

36. Azhari, A., Golestani-Fard, F., and Sarpoolaky, H., "Effect of nano iron oxide as an additive on phase and microstructural evolution of Mag-Chrome refractory matrix", *J. Euro. Ceram. Soc.*, 29, pp.2679–2684 (2009).
37. Satpathy, S., "Influence of nano-Fe<sub>2</sub>O<sub>3</sub> on the microstructure and property development of silica brick", M. Tech Thesis, NIT-Rourkela (2008).
38. Karamian, E., and Monshi, A., "Influence of additives on nano-SiC whisker formation in alumina silicate–SiC–C monolithic refractories", *Ceram. Int.*, 36, pp.811–816 (2010).
39. Otroj, S., Sagaeian, A., Daghighi, A., and Ali Nemati, A., "The effect of nano-size additives on the electrical conductivity of matrix suspension and properties of self-flowing low-cement high alumina refractory castables", *Ceram. Int.*, 36, pp.1411-1416 (2010).
40. Mukhopadhyay, S., Das Poddar, P.K. "Role of nanocrystalline spinel additive on the properties of low cement castable refractories", *Materials and manufacturing processes*, 21, pp.669 – 675 (2006).
41. Ghosh, S., Maiti, T., Sen, S. and Mukhopadhyay, S. "Influence of gel-derived nanocrystalline spinel in a high alumina castable: Part 1", *Ceram. Int.*, 31, pp.333-347 (2005).
42. Mukhopadhyay, S., Pal, P. Nag, B., and Jana, P., "Influence of gel-derived nanocrystalline spinel in a high alumina castable: Part 2", *Ceram. Int.*, 33, pp.175-186 (2007).
43. Ewais, E.M.M., "Carbon based refractories", *J. Ceram. Soc. Jpn.*, 112, pp.517-532 (2004).
44. Quintela, MA., Santos, FD., Pessoa CA., Rodrigues, JA., and Pandolfelli, VC., "MgO-C refractories for steel ladles slag line", *Refractories Applications and news*, 11, pp.15-19 (2006).
45. Buchener, G., and Piker, S., "New high performance refractories for BOF vessels", *Veitsch-Radex Rundschau*, 2, pp.3-14 (1996).
46. Ruh, E., "Refractories: Magnesia–Carbon Refractories, History, Development, Types and Applications", *International Ceramic Monographs*, 1, pp.772-793 (1994).

47. Hashemi, B., Nemati, Z.A., and Faghihi-Sani, M.A., "Effects of resin and graphite content on density and oxidation behaviour of MgO-C refractory bricks", *Ceram. Int.*, 32, pp.313-319 (2006).
48. Kido, N., Yamamoto, K., and Kamiide, M., "Carbon nanofiber- a new trial for magnesia based bricks", *Proc. UNITECR'03*, Osaka, Japan, pp.264-267 (2003).
49. Yamaguchi, A., "Control of oxidation-reduction in MgO-C refractories", *Taikabutsu Overseas*, 4, pp.32-36 (1984).
50. Missen, R.W. and Mims, C.A., "Introduction to chemical reaction engineering and kinetics", John Wiley & Sons Inc., New York, pp.224 (1999).
51. Anan, K., "Wear of refractories in basic oxygen furnaces (BOF)", *Taikabutsu Overseas*, 21, pp.241-246 (2001).
52. Maekawa, A., Geji, M., Tanaka, M., Kitai, T., and Furukawa, K., "Influence of impurities in fused magnesia on the properties of MgO-C bricks", *TARJ*, 21, pp.74 (2001).
53. Minami, Y., Fuchimoto, H., Hokii, T., and Asano, K., "Effect of MgO purity on the corrosion resistance of MgO-C bricks against high temperature iron oxide slag", *TARJ*, 21, pp.212 (2001).
54. Tanaka, M., Maekawa, A., Hokii, T., Asano, K., and Ohtsuka, K., "Relationship between MgO aggregate purity and properties of MgO-C brick after firing in a reducing atmosphere", *TARJ*, 21, pp.215 (2001).
55. Staron, J. and Palco, S., "Production technology of magnesia clinker", *Am. Ceram. Soc. Bull.*, 72, pp.83-87 (1993).
56. Yoshida, A., "On the present status of seawater magnesia manufacturing", *TARJ*, 25, pp.89-99 (2005).
57. Ishii, H., Tsuchiya, I., Oguchi, Y., Kawamaki, T., and Takahashi, H., "Behaviour of impurities in magnesia-carbon brick at high temperatures", *Taikabutsu Overseas*, 10, pp.3-8 (1990).
58. Nameishi, N., Ishibashi, T., Matsumura, T., Hosokawa, K., and Tsuchinai, A., *Taikabutsu*, 32, pp.583-587 (1980).
59. Matsuo, A., Miyagawa, S., Ogasawara, K., Yokoi, M., Uchimura, R., and Kumagai, M., *Taikabutsu*, 36, pp.644-647 (1984).

60. Matsui, K., and Kawano, F., "Effect of impurities in magnesia on reaction between magnesia clinker and carbon", *Taikabutsu Overseas*, 14, pp.3-12 (1994).
61. Tanaka, S., Okajima, S., Sugimoto, T., and Fujio, M., *Taikabutsu*, 35, pp.643-646 (1983).
62. Rita, K., John, S., and Veena, S., "Role of ash impurities in the depletion of carbon from alumina-graphite mixtures in to liquid iron", *ISIJ International*, 47, pp.282-288 (2007).
63. Sakaguchi, M., Ishii, H., Aratani, K., and Oguchi, Y., "Effect of graphite particle size on properties of MgO-C bricks", *Taikabutsu Overseas*, 13, pp.27-29 (1993).
64. Yamaguchi, A., and Yu, J., *Taikabutsu*, 44, pp.700-707 (1992).
65. Nishimura, D., "Technical trends of phenolics for Japanese refractories", *Taikabutsu Overseas*, 15, 10-14 (1995).
66. Gokce, A.S., Gurcan, C., Ozgen, S., and Aydin, S., "The effect of antioxidants on the oxidation behaviour of magnesia-carbon refractory bricks", *Ceram. Int.*, 34, pp. 323-330 (2008).
67. Zhang, S., Marriott, N.J., and Lee, W.E., "Thermo chemistry and microstructures of MgO-C refractories containing various antioxidants", *J. Euro. Ceram. Soc.*, 21, pp.1037-1047 (2001).
68. Nandy, S.K., Ghosh, N.K., and Das, G.C., "Evaluation of critical properties for magnesia carbon with addition of metallic", *Proc. UNITECR'05*, Orlando, Florida, USA, pp.1-5 (2005).
69. Ye, F., and Rigaud, M., "Effects of boron bearing additives on oxidation and corrosion resistance of doloma-based carbon bonded refractories", *Proc. UNITECR'97*, New Orleans, USA, pp.807-815 (1997).
70. Onoda, K., Hashimoto, S., and Yamaguchi, A., "Comparison of additives in MgO-C refractories", *TARJ*, 20, pp.68 (2000).
71. Imaeada, T., Koide, K., Morimoto, S., and Koike, Y., "Effect of boron containing additives on magnesia-carbon bricks", *TARJ*, 21, pp.216 (2001).
72. Guha, J.P., and Smith, J.D., "Reaction chemistry and microstructure development of MgO-C refractories containing metal antioxidants", *Proc. UNITECR'05*, Orlando, USA, pp.97-99 (2005).



73. Yamaguchi, A., "Behaviours of SiC and Al added to carbon containing refractories", Taikabutsu Overseas, 4, pp.14-18 (1984).
74. Matsumura, T., Uto, S., Hosokawa, K., and Geji, M., "Properties of magnesia carbon bricks containing aluminum or aluminum alloys", Taikabutsu Overseas, 8, pp.24-26 (1988).
75. Hanagiri, S., Harada, T., Aso, S., Fujihara, S., Yasui, H., Takanaga, S., Takahashi, H., and Wattanabe, A., "Effects of the addition of metal and  $\text{CaB}_6$  to magnesia carbon bricks for converters", Taikabutsu Overseas, 13, pp.20-27 (1993).
76. Yamaguchi, A., and Tanaka, H., "Behaviour and effects of  $\text{ZrB}_2$  added to carbon-containing refractories", Taikabutsu Overseas, 15, pp.3-9 (1995).
77. Suruga, T., "Effect of Mg-B metal addition to MgO-C bricks", Taikabutsu Overseas, 15, pp.25-31 (1995).
78. Karakus, M., Smith, J.D., Moore, R.E., "Mineralogy of the carbon containing steel making refractories", Proc. UNITECR'97, New Orleans, USA, pp.745-753 (1997).
79. Hunold, K., Ollig, M., Potschke, J., and Rymon-Lipinski, T., "The effect of  $\text{B}_4\text{C}$  and  $\text{CaB}_6$  additions in MgO-C bricks", Proc. UNITECR'97, New Orleans, USA, pp.789-797 (1997).
80. Higuchi, M., Hashimoto, S., and Yamaguchi, A., "Effect of added  $\text{CrB}_2$  in MgO-C refractories", TARJ, 21, pp.69 (2001).
81. Aneziris, C.G., Hubalkova, J., and Barabas, R., "Microstructure evaluation of MgO-C refractories with  $\text{TiO}_2$ - and Al-additions", J. Euro. Ceram. Soc., 27, 73-78 (2007).
82. Mori, J., Watanabe, N., Yoshimura, M., and Oguchi, Y., and Kawakami, T., "Material design of monolithic refractories for steel ladle", Am. Ceram. Soc. Bull., 69, pp.1172-1176 (1990).
83. Baudin, C., Martinez, R., and Pena, P., "High-temperature mechanical behaviour of stoichiometric magnesium aluminate spinel", J. Am. Ceram. Soc., 78, pp.1857-1862 (1995).
84. A. Ghosh, S. K. Das, J. R. Biswas, H. S. Tripathi, G. Banerjee, "The effect of ZnO addition on the densification and properties of magnesium aluminate spinel" Ceram. Inter., 26, pp. 605-608 (2000).

85. L. N. Satapathy, "High Temperature Deformation Behaviour of a High Purity  $\text{Al}_2\text{O}_3$  Reinforced with Isolated Second Phases of Spinel ( $\text{MgAl}_2\text{O}_4$ ), YAG ( $\text{Y}_3\text{Al}_5\text{O}_{12}$ ) and Zirconia ( $\text{t-ZrO}_2$ )" Transactions of the INDIAN CERAMIC SOCIETY, 65, pp. 145 -156 (2006).
86. B. B. Sahu, B. K. Panda, B. Mishra, N. Sahoo, J. N. Tiwari, "Mechanism of spinelisation and the role of sesqui-oxides on the properties of synthetically prepared refractory materials"-Proceedings in International seminar on ceramics, CeraTec, pp.-47-48 (2007).
87. Gonsalves, G.E., Duarte, A.K., Brant, P.O.R.C., "Magnesia-spinel brick for cement rotary kilns", Am. Ceram. Soc. Bull., 72, pp.49-54 (1993).
88. Marra, R.A., Haling, S., and Soora, S., "Compositional variables and their effect on steel slag resistance and hot strength of high alumina-spinel castables", Proc. UNITECR'95, Kyoto, Japan, Vol.2, pp.675-682 (1995).
89. Nagai, B., Matsumoto, O., Isobe, T., and Nishiumi, Y., "Wear mechanism of castable for steel ladle by slag", Taikabutsu Overseas, 12, pp.15-20 (1992).
90. S. Mukhopadhyay, T.K. Pal, P.K. DasPoddar, "Improvement of corrosion resistance of spinel-bonded castables to converter slag" Ceram. Inter., 35, pp. 373-380 (2009).
91. Vance, M.W., Krichbaum, G.W., Henrichsen, R-A., MacZura, G., Moody, K.J., and Munding, S., "Influence of spinel additives on high alumina/spinel castables", Bull. AM. Ceram. Soc., 73, pp.70-74 (1994).
92. Díaz, L.A., Torrecillas, R., de Aza, A.H., and Pena, P., "Effect of spinel content on slag attack resistance of high alumina refractory castables", J. Euro. Ceram. Soc., 27, pp.4623-4631 (2007).
93. Nakagawa Z, Enomoto N, Yi IS, Asano K. Effect of corundum/periclase sizes on expansion behaviour during synthesis of spinel. Proc. UNITECR'95, Kyoto, Japan, pp. 379–386 (1995).
94. Lee, W.E., Argent, B.B. and Zhang, S., "Complex phase equilibrium in refractories design and use", J. Am. Ceram. Soc., 85, pp.2911-2918 (2002).
95. Lee, W.E., and Moore, R.E., "Evolution of *in Situ* refractories in the 20th Century", J. Amer. Ceram. Soc., 81, pp.1385 – 1410 (2005).

96. Das, T. and Toledo, O.D., "Development of magnesia-spinel-carbon brick for ladles of secondary metallurgy, Proc. UNITECR'95, Kyoto, Japan, pp. 278-283 (1995).
97. Aksel, C. and Warren, P.D., "Thermal shock parameters [ $R$ ,  $R''$  and  $R''''$ ]] of magnesia-spinel composites", J. Euro. Ceram. Soc., 23, pp.301-308 (2003).
98. Lee, W.E., and Zhang, S., "Melt corrosion of oxide and oxide-carbon refractories", International Materials Reviews, 44, pp.77-104 (1999).
99. Lee, W.E., and Zhang, S., "Direct and indirect slag corrosion of oxide and oxide-c refractories", VII International Conference on Molten Slags Fluxes and Salts, The South African Institute of Mining and Metallurgy, pp.309-320 (2004).
100. Cooper, A.R., "Kinetics of refractory corrosion", Ceramic Engineering and Science Proceedings", 2, pp.1063-1086 (1982).
101. Taira, S., Nakashima, K., and Mori, K., "Kinetic behavior of dissolution of sintered alumina into  $\text{CaO-SiO}_2\text{-Al}_2\text{O}_3$  slags", ISIJ International, 33, pp.116-123 (1993).
102. Arasu, V.C., Das, S., Adak, S., and Chattopadhyay, A.K., "Effect of nano-titania addition on the properties of magnesia carbon system", Proc. UNITECR'09, Salvador, Brazil, Article ID.079 (2009).
103. Mukherjee, S.G. and Samaddar, B.N., "Spinel formation from co-precipitated hydroxides of aluminium and magnesium", Trans. Indian Ceramic Society., 25, pp.4 (1996).
104. Sarkar, R., Das, K., Das, S.K. and Banerjee, G., "Development of magnesium aluminate spinel by solid oxide reaction", Proc. UNITECR'97, New Orleans, USA, Vol.II, pp.1053-1058 (1997).
105. Sarkar, R., Das, S.K. and Banerjee, G., "Calcination effect on magnesium hydroxide and aluminium hydroxide for the development of magnesium aluminate spinel", Ceram. Int., 26, pp.25-28 (2000).
106. Sarkar, R., Das, S.K. and Banerjee, G., "Densification study of attritor milled magnesium aluminate spinel", Trans. Indian Ceramic Society., 58, pp.92-94 & 103 (1999).
107. Sarkar, R., Das, S.K. and Banerjee, G., "Effect of attritor milling on the densification of magnesium aluminate spinel", Ceram. Int., 25, pp.485-489 (1999).

108. Sarkar, R. and Banerjee, G., "Effect of compositional variation and fineness on the densification of MgO–Al<sub>2</sub>O<sub>3</sub> compacts", J. Euro. Ceram. Soc., 19, pp.2893-2899 (1999).
109. Sarkar, R. and Banerjee, G., "Spinellization of magnesium and aluminium hydroxides with pressure and temperature", Trans. Indian Ceramic Society., 58, pp.5-6 (1999).
110. Sarkar, R. and Banerjee, G., "Single stage densification study of different magnesium aluminates in presence of additives", Industrial Ceramics, 20, pp.1-4 (2000).
111. Sarkar, R. and Banerjee, G., "Effect of additives of TiO<sub>2</sub> on reaction sintered MgO–Al<sub>2</sub>O<sub>3</sub> spinels", J. Euro. Ceram. Soc., 20, pp.2133-2141 (2000).
112. Sarkar, R. and Banerjee, G., "Effect of oxide additions on the densification of spinels", Proc. of 4<sup>th</sup> Indian Industrial Refractory Congress, Vol.II, pp.111-116 (2000).
113. H .S. Tripathi, B. Mukherjee, S. Das, M.K. Haldar, S.K. Das, A. Ghosh, "Synthesis and densification of magnesium aluminate spinel: effect of MgO reactivity" Ceram. Inter., 29, pp. 915–918 (2003).
114. Saberi, A., Golestani-Fard, F., Willert-Porada, M., Negahdari, Z., Liebscher, C., and Gossler, B., "Chemical synthesis of nanocrystalline magnesium aluminate spinel via nitrate-citrate combustion route", J. Alloys. Compound, 462, pp.142-146 (2008).
115. Behera, S.K., Barpanda, P., Pratihari, S.K., and Bhattacharya, S., "Synthesis of magnesium-alumina spinel from auto ignition of citrate-nitrate gel", Mater. Lett., 58, pp.1451-1455 (2004).
116. Zhang, H., Jia, X., Liu, Z., and Li, Z., "The low temperature preparation of nanocrystalline MgAl<sub>2</sub>O<sub>4</sub> spinel by citrate sol–gel process", Mater. Lett., 58, pp.1625 – 1628 (2004).
117. Zawrah, M.F., "Investigation of lattice constant, sintering and properties of nano Mg–Al spinels", Mat. Sci. Engg., A382, pp.362-370 (2004).
118. Zawrah, M.F., Hamaad, H., and Meky, S., "Synthesis and characterization of nano MgAl<sub>2</sub>O<sub>4</sub> spinel by the co-precipitated method", Ceram. Inter., 33, pp.969–978 (2007).

119. Paulick, L.A., et al., "Ceramic powders from alkoxide precursors, *Advances in ceramics*", Ed. By, G.L. Messing et al., Am. Ceram. Soc., 21, pp.99-107 (1988).
120. Saberi, A., Golestani-Fard, F., Willert-Porada, M., Negahdari, Z., Liebscher, C., and Gossler, B., "A novel approach to synthesis of nanosize  $\text{MgAl}_2\text{O}_4$  spinel powder through sol-gel citrate technique and subsequent heat treatment", *Ceram. Int.*, 35, pp.933-937 (2009).
121. Ganesh, I., Johnson, R., Rao, G.V.N., Mahajan, Y.R., Madavendra, S.S., and Reddy, B.M., "Microwave assisted combustion synthesis of nano-crystalline  $\text{MgAl}_2\text{O}_4$  spinel powder", *Ceram. Int.*, 31, pp.67-74 (2005).
122. Wang, C.T., Lin, L.S., and Yang, S.J., "Preparation of  $\text{MgAl}_2\text{O}_4$  spinel powders via freeze-drying of alkoxide precursors", *J. Am. Ceram. Soc.*, 75, pp.2240-2243 (1992).
123. Bickmore, C.R., Walder, K.F., and Treadwell, D.R., "Ultra fine spinel powders by flame spray pyrolysis of a magnesium aluminium double alkoxide", *J. Am. Ceram. Soc.*, 79, pp.1419-1423 (1996).
124. Sahoo, N., Panda, B.K., Tiwari, JN and Chaudhuri, SK., "Some aspects of corrosion of magnesia carbon, alumina magnesia carbon and alumina-silicon-carbide carbon refractory bricks", Workshop on corrosion of refractories in iron & steel making, Aug.'06, Indian Ceramic Society, Jamshedpur, pp.1-7 (2006).
125. Annual Book of ASTM Standards, Vol.15.01, 1999. ASTM C133-97: Tests methods for cold crushing strength and modulus of rupture of refractories.
126. Cullity, B.D., and Stock, S.R., *Elements of X-Ray Diffraction*, 3<sup>rd</sup> Ed., Prentice-Hall Inc., pp. 167-171 (2001).
127. Amin, MH., Amin-Ebrahimabadi, M. and Rahimipour, MR., "The effect of nanosized carbon black on the physical and thermomechanical properties of  $\text{Al}_2\text{O}_3$ -SiC-SiO<sub>2</sub>-C composite", *J. of Nanomaterials*, (2009), Article ID: 325674, 5 pages, (doi:10.1155/2009/325674),  
<http://www.hindawi.com/journals/jnm/2009/325674.html>.
128. Carniglia, S.C. and Barna, G.L., "Handbook of industrial refractories technology: Principles, types, properties and applications", Noyes publication, pp.442-443 (1992).

129. Nomura, O., Tada, H., Torigoe, A., and Hoshiyama, Y., “Environmentally friendly carbon containing refractories – Fumeless products”, *TARJ*, 20, pp.254-256 (2000).
130. Sen, P., Prasad, B., Sahu, J.K. Sahoo, N., and Tiwari, J.N., Effect of nano-oxides and anti-oxidants on corrosion and erosion behaviour of submerged nozzle for longer sequence casting of steel, *Proc. UNITECR’09*, Salvador, Brazil, Article ID.021 (2009).
131. Sarpoolaky, H., Zhang, S., Argent, B.B., and Lee, W.E., “Influence of grain phase on slag corrosion of low-cement castable refractories”, *J. Am. Ceram. Soc.*, 84, pp.426-434 (2001).
132. T. Nishitani, Application of the alumina – spinel castable for BOF ladle, *Proc. UNITECR’89*, Anaheim, USA, pp.529-540 (1989).
133. Yamamura, T., Hamazaki, Y., Kaneshige, T., Toyoda, T., Nishi, M., and Kato, H., “Development of alumina-spinel castable refractories for steel teeming ladle”, *Taikabutsu*, 42, pp.427-434 (1990).
134. Yamamura, T., Kubota, Y., Kaneshige, T., and Nanba, M., “Effect of spinel clinker composition on properties of alumina-spinel castable”, *Taikabutsu*, 44, pp.404-412 (1992).
135. H. Zhang, Z. He, M. Gan, B. Liu, Effect of nano-CaCO<sub>3</sub> addition on mechanical properties and microstructure of corundum based castable, *Proc. UNITECR’09*, Salvador, Brazil, Article ID.131 (2009).
136. Bavand-Vandchali, M., Golestani-Fard, F., Sarpoolaky, H., Rezaie, H.R., and Aneziris, C.G., “Corrosion study of spinel bonded MgO-C refractories by silicate slags, 51<sup>st</sup> International colloquium on refractories”, 2008, Aachen, Germany, pp.110-113 (2008).

### **Curriculum Vitae**

**Name** : Mrs. Rashmi Rekha Das  
**Date of Birth** : 25<sup>th</sup> December 1978  
**Sex** : Female  
**Marital Status** : Married  
**Nationality** : Indian  
**Address for Communication** : Mrs. Rashmi Rekha Das  
Qr. No: P-27, TRL Township  
Belpahar (Post), Jharsuguda (District)  
Orissa – 768 218

**Education Qualification** :

Examination	Board	Year of Passing	Marks (%)	Division
AICeram ( <i>Equivalent to B.Tech -Ceramics</i> )	Indian Ceramic Society	2006	63.79	First
Diploma (Ceramic Tech.,)	SCTE & VT	1999	74.21	First (Hons.)
SSLC	CBSE	1994	76.40	First

**Industrial Experience** :

- (i) Working as Officer (R&D) in M/s. Tata Refractories Ltd., Orissa, India since Dec'2004 to till date (Domain: Testing and instrumentation, New product development).
- (ii) Served in M/s. Tata Refractories Ltd., Orissa, India as Officer (R&D) from August 2001 to December.2003 (Domain: In-process quality control). .
- (iii) Apprenticeship Trainee at M/s. NALCO, Orissa, India from January 2001 to August 2001.
- (iv) Technical training on application of refractories in steel plant at M/s.TISCO through SNTI.

**Languages Known** : Fluent in reading, writing and speaking  
English, Hindi, Oriya

**Extra Curricular Activities** : Sketching, Singing, Playing badminton and  
community development work

**Computer Knowledge** : Well versed with personal computer

### **Publications resulting from the M. Tech (R) work**

1. Rashmi R Das, Bibhuti B. Nayak, S. Adak, A. K. Chattopadhyay, "Effect of spinel addition in MgO-C refractory for slag zone of steel ladle", Technical proceedings in IREFCON 10, pp-155-159 (2010).
2. Rashmi R Das, S. Adak, A. K. Chattopadhyay, Bibhuti B. Nayak, "Influence of nanocrystalline MgAl<sub>2</sub>O<sub>4</sub> spinel addition on the properties of MgO-C refractories" (Communicated in Materials and Manufacturing Processes).

**(Rashmi Rekha Das)**